



# Blast loading effects on UHPFRC structural elements: a review

Rizwanullah<sup>1</sup> · H. K. Sharma<sup>1</sup>

Received: 21 June 2022 / Accepted: 16 September 2022 / Published online: 30 September 2022  
© Springer Nature Switzerland AG 2022

## Abstract

High-strain-rate loadings, including blast loads acting on the structures, have become a matter of deep concern, primarily due to increased terrorist activities, which pose a severe threat to the lives of the people and facilities. With increasing terrorist activities, people living in the targeted areas are at stake. The compressive strength of ultra-high-performance fiber-reinforced concrete (UHPFRC) is 4–5 times that of ordinary strength concrete. It exhibits exceptional resistance to fragmentation and energy absorption capacity, enhancing the ability to disseminate higher blast energy and improved behavior than conventional concrete. The present paper discusses an exhaustive review of published work on the influence of blast loading on UHPFRC elements in an attempt to comprehensively provide detailed information to researchers. The typical observations and critical analysis may be used to identify the gaps in the published work to carry forward the research work in the area.

**Keywords** Blast loading · Blast wave · Peak pressure · Impulse · Wave parameters · UHPFRC

## Introduction

The response of structural systems subjected to blast loading is of paramount importance because of the fact that it involves material and geometric non-linearities, loading rate-based material characteristics and structural deformations, which are time dependent. Complexities arise because the structural and material nonlinear characteristics have led to various approximations and assumptions to analyze the model in a simplified manner. Localized failure of few structural elements causes a progressive collapse following a severe explosive loading on the structural system. The localized failures initiate a chain reaction which could cause a total destruction or collapse of the structure. Military bombing including disasters, in the recent past, has created the requirement for a detailed study of the performance of structural systems impacted by blast loads. Architectural planning, design and construction of public structures have drawn significant attentiveness of architects and civil

engineers world over, to ensure avoidance of structures adjoining to explosions and blasts.

The ordinary strength concrete (OSC) is not capable of withstanding high-strain-rate loading and fails explosively causing instantaneous collapse of the structure. Ultra-high-performance fiber-reinforced concrete (UHPFRC) matrix, a new and innovative material, is being utilized by the construction industry nowadays for various structural elements, because of the fact that it possesses high compressive, tensile and flexural characteristics and is a very dense composite having low permeability due to its minimal disconnected structure.

Significant studies were conducted by various researchers to experimentally and analytically evaluate UHPFRC structural systems under explosive loading in different environments. It was observed that UHPFRC can support more than four times more impulsive loads than OSC. Studies on columns, slabs, beams, etc., constructed using UHPFRC demonstrated significant improvement in static and blast capacities. It was also seen that UHPFRC plates out performed OSC slabs after blast. Although numerous experimental studies have been done to examine performance of UHPFRC subjected to impact loading, very few investigations have been published on studies pertaining to performance of this noble material when subjected to blast loads probably because of obvious reasons of limited facilities, exorbitantly

---

✉ Rizwanullah  
rizwan\_6170002@nitkr.ac.in

H. K. Sharma  
hksharma1010@yahoo.co.in

<sup>1</sup> Department of Civil Engineering, National Institute of Technology, Kurukshetra, Haryana, India

expensive testing, restrictions on use of explosives due to security reasons, strategic importance of research, etc.

## New-generation UHPFRC

UHPFRC illustrates very strong strength characteristics, ductility, durability and blast and impact resistant capabilities when compared with OSC. Because of its extraordinary structural properties, like high tensile, flexural, and shear strengths, conventional reinforcement, which is not environmentally friendly, can be partially or completely replaced. Figure 1 demonstrates stress–strain characteristics of UHPFRC and normal strength concrete (NSC), commonly known as OSC, in compression and tension, respectively. Developed by Richard et al. in 1990s as a new class of composite, UHPFRC is associated with a brand called Ductal. Bouygues et al. [1] developed and published the product called reactive powder concrete (RPC), traditionally known as UHPFRC, which is a cementitious material that constitutes cement, silica fume, sand, silica flour, superplasticizer, high steel fibers, and water. UHPFRC, a self-compacting type of concrete, possesses compressive and flexural strengths of the order of 160–200 and 30–40 MPa, respectively. It has a large energy absorption capacity, fragmentation resistance, and excellent ability to perform under explosion, shock, and impact loads. The flexural toughness is more than 200 times that of OSC. UHPFRC, which is a next generation composite, also possess an extraordinary durability property as compared to OSC.

However, as UHPFRC is an expensive composite than OSC which needs to be designed and developed very precisely for its usage in structures of strategic significance. Table 1 demonstrates details of constituent materials used by various investigators in developing UHPFRC during the past 17 years to achieve a composite of higher strength values. Ultra-high-performance fiber-reinforced concrete (UHPFRC) is associated with a brand called Ductal. Bouygues, Rhodia, and Lafarge [2] first developed and published the

product reactive powder concrete (RPC) which is commonly termed as UHPFRC. UHPFRC is a cementitious material that constitutes cement, silica fume, sand, silica flour, superplasticizer, high steel fibers, and water. UHPFRC is a self-compacting kind of concrete and possesses compressive and flexural strengths of 160–200 and 30–40 MPa, respectively. It has a large energy absorption capacity, fragmentation resistance, and excellent ability to perform under explosion, shock, and impact loads. The flexural toughness is more than 200 times that of OSC. UHPFRC, which is a next generation composite, also possess an extraordinary durability property compared to OSC.

Assessment of performance against blast loading due to increased terror attacks and instant explosions has become an inevitable component in the analysis and design of structures of strategic importance. Progressive type of damage caused due to local failure of few structural elements may cause catastrophic collapse of additional building components and loss of life. UHPFRC is nowadays widely studied by many researchers to eliminate blast loading effects on buildings. Computer modeling and FE numerical analysis are commonly used to simulate blast loading effects on structures. UHPFRC is extensively used in high-performance structures exposed to ballistic loads, earthquakes and blast loads.

The militant attack and fatalities, which occurred in the country during 2009–2017, are illustrated in Figs. 2 and 3. However, several explosions took place by terrorists' activities globally. The major recent examples are the blast event in Texas City explosion, USA (April 16, 1947), Iri station explosion (November 11, 1977), Beirut (August 4, 2020), Barajas International Airport, Lac-Megantic explosion, Canada (July 6, 2013), Boston Marathon bombing, USA (April 15, 2013), Marriott hotel bombing, Islamabad, Pakistan (September 20, 2008), Khobar towers bombing, Saudi Arabia (June 25, 1996), Madrid, Spain (December 30, 2006), Arndale Shopping Centre, Manchester, United Kingdom (June 15, 1996), Central Bank of Sri Lanka (1996), London Docklands (1996), Alfred P. Murrah Building, Oklahoma

**Fig. 1** Stress versus strain characteristics of UHPFRC and normal strength concrete (NSC) in compression and tension (Wu et al. [1])

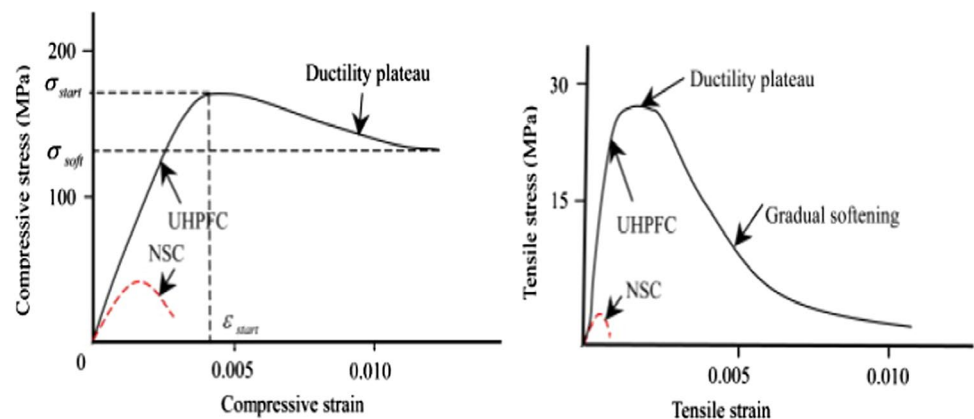
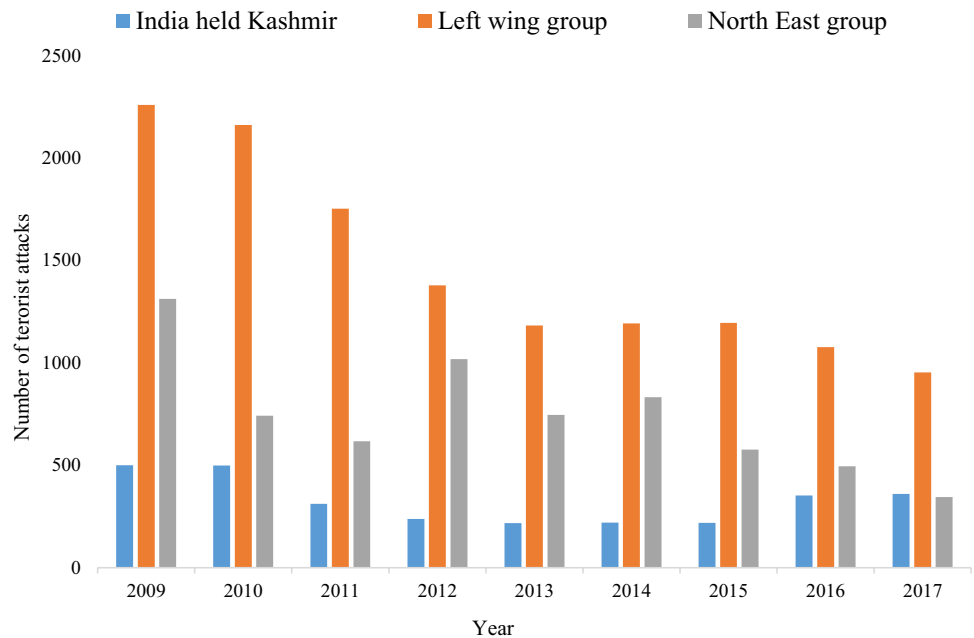


**Table 1** Composition used by various researchers for production of UHPFRC

| S. No | References         | Composition (kg/m <sup>3</sup> ) |        |     |          |      |                  |         |       | Strength (MPa) |            |
|-------|--------------------|----------------------------------|--------|-----|----------|------|------------------|---------|-------|----------------|------------|
|       |                    | C                                | SF     | FA  | SS       | GGBS | S <sub>t</sub> F | W       | SP    | CS             | FS         |
| 1     | Habel et al. [3]   | 1050                             | 275    | –   | 730      | –    | 470              | 190     | 35    | 175            | 13         |
| 2     | Graybeal [4]       | 710                              | 230    | –   | 1020     | –    | 156              | 110     | 31    | 126–193        | –          |
| 3     | Katrin Habel [5]   | 967                              | 251    | –   | 675      | –    | 430              | 244     | 35    | –              | 11         |
| 4     | Hassan et al. [6]  | 657                              | 119    | –   | 1051     | 418  | 157              | 185     | 40    | 145.96–150.56  | 8.97–9.07  |
| 5     | Tayeh et al. [7]   | 610–1390                         | 50–334 | –   | 490–1390 | –    | 40–250           | 126–261 | 9–71  | –              | 10–14      |
| 6     | Li et al. [8]      | 680                              | 204    | –   | 1130     | –    | 156              | 150     | 44    | 128.9          | 30         |
| 7     | Li et el. [9]      | 750                              | 415    | –   | 1030     | –    | –                | 190     | 16    | 175            | 30         |
| 8     | Li et al. [10]     | 1155                             | 437    | –   | 178      | –    | –                | 305     | 40    | –              | –          |
| 9     | Mao et al. [11]    | 657                              | 119    | –   | 1051     | 418  | 157              | 185     | 40    | 170–190        | 10–13      |
| 10    | Xu et al. [12]     | 995                              | 229    | –   | 1051     | –    | –                | 16      | –     | –              | –          |
| 11    | Su et al. [13]     | 750                              | 225    | –   | 1220     | –    | 60               | 190     | 16    | –              | –          |
| 12    | Kang et al., [14]  | 741                              | 185    | –   | 815      | –    | 151              | 185     | 9     | 155–167        | –          |
| 13    | Turker et al. [15] | 690                              | 138    | –   | 1050     | 276  | 33               | 199     | 17.25 | 145            | 9.32–11.18 |
| 14    | Song et al. [16]   | 750                              | 144    | 200 | 990      | –    | 39               | 190     | 35    | –              | –          |
| 15    | Chu et al. [17]    | 449                              | 192    | 641 | –        | –    | 157              | 226     | 38    | –              | –          |

C Cement, SF Silica fume, FA Fly Ash, SS Silica sand, GGBS Ground granulated blast furnace slag, S<sub>t</sub>F steel fiber, W Water, SP Superplasticizer, CS Compressive strength, FS Flexural strength

**Fig. 2** Insurgent and militant attacks during 2009–2017 [18]



City (April 19, 1995), and World Trade Centre in New York City in Washington on September 11, 2001, The Shijiazhuang bombings, China, March 16, 2001, AZF chemical factory, France, September 21, 2001. These activities illustrated the extent of threat of terrorist activities to understand the importance of design of blast-resistant structures to provide safe response of structure to minimize the negative consequence of blast loading. Figure 4 demonstrates distribution frequency of incidents that took place across various

regions. Latin America region was observed to be the worst affected region for terrorist events.

Blast loads in the form of explosion act in the form of moving pressure waves on the system introduces dynamic forces in the structure due to which structures dynamic response causes a high strain-rate change in various material and structural characteristics. The rapid release of stored chemical energy generated during an explosion releases significant amount of thermal radiations, while

**Fig. 3** No. of destroyed properties by militants during 1990–1999 [18]

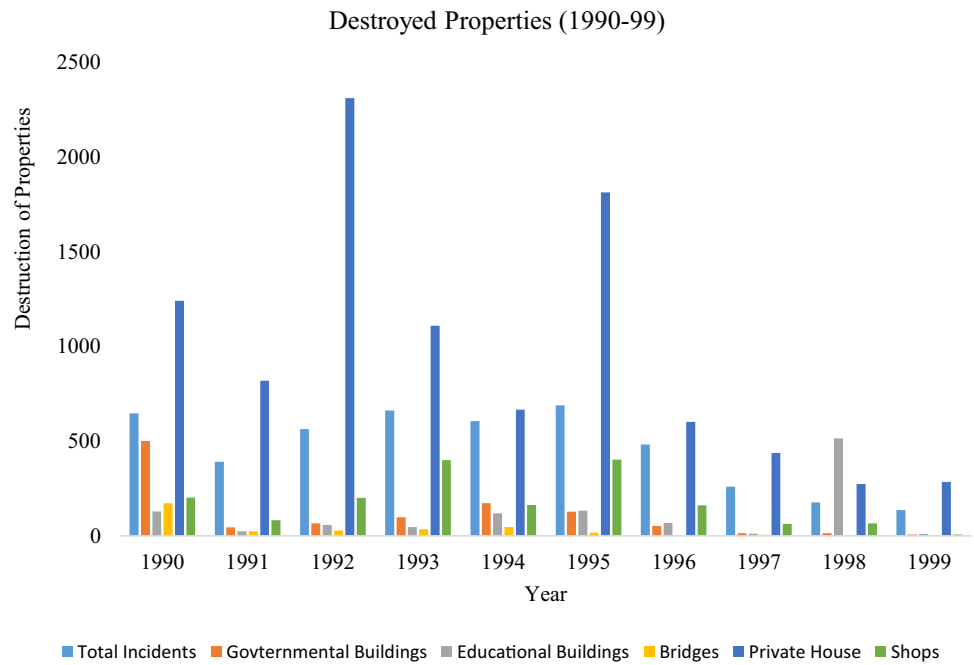
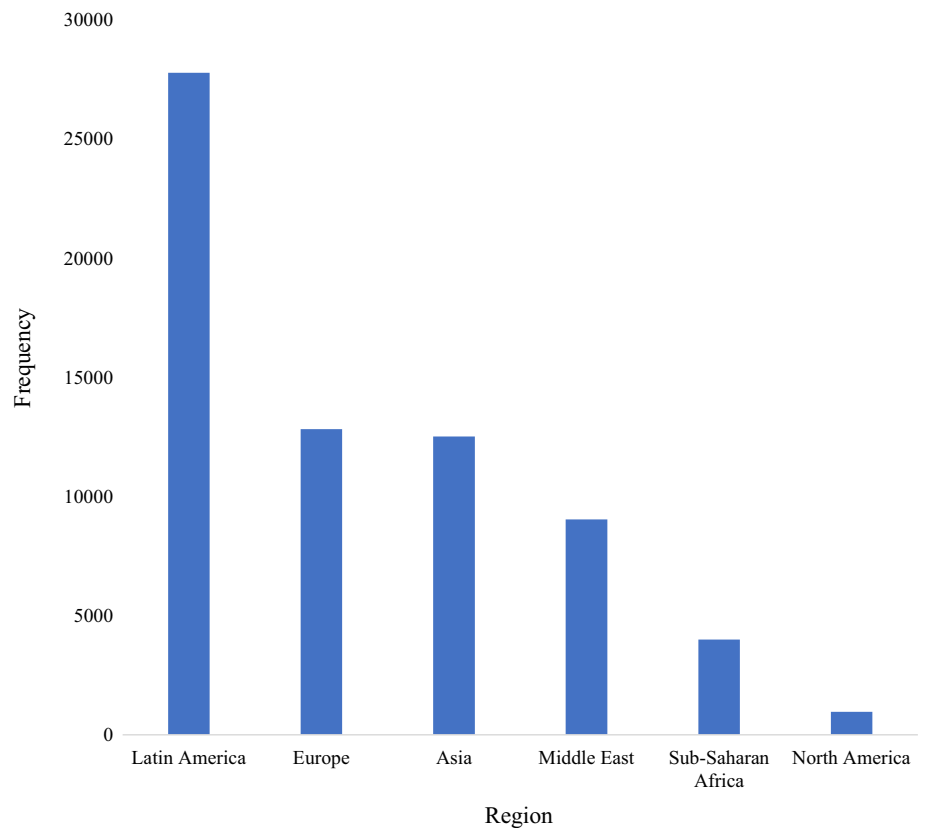


**Fig. 4** Distribution of events as per region [19]



the rest is transmitted as shock waves due to combination of ground shock and air blast. The consequence of an air blast is ambient over-pressure or incident pressure,

created by the air blast traveling at supersonic speed through the air thereby compressing air molecules along its path.

### Explosion effects

Explosions produce a very high magnitude of dynamic loads greater than the loads at the start, for which the structural elements are to be studied and protected by blast loads. Figure 5 depicts measures that can be taken to improve a building's blast resistance.

The significant consequence of an air blast is ambient over-pressure or incident pressure, created by the air blast traveling at supersonic speed through the air, compressing air molecules along its path. The dynamic pressure or drag load is a secondary result of the air blast. When a shock wave hits a firm object, such as a building wall, it reflects the overpressure by a factor ranging from 2 to 13. The air explosion may enter the structure through wall openings, broken doors and windows, causing damage to structural elements, including floor slabs and partitions. Due to their interaction with various surfaces, the shock waves diffract, increasing or decreasing pressure. Overpressure eventually affects the entire structure. The pressures fall exponentially with radial distance from the blast's epicenter and time, measured in milliseconds. Some building features, such as re-entrant corners, may cause diffraction in the pressure waves, limiting the air blast and extending its duration. The pressure created by the shock wave eventually becomes negative, resulting in a vacuum pressure that introduces suction forces. Air rushes in at a high velocity due to the negative pressure, propelling debris formed by the blast. Dynamic pressure or drag loading refers to the forces acting on the structure. Due to the blast energy transferred to the ground, vibrations similar to high-intensity, short-duration ( $t_a$ ) earthquakes are formed in the case

of an external explosion. The parameters of a typical blast wave are represented in Fig. 6. Table 2 shows the values of additional damages caused by the blast and the incident overpressure.

The positive incident pressure decreases exponentially, as shown in Fig. 6. Karlos and Solomos [22] proposed Friedlander's equation, which is widely used to solve the rate of decrease of pressure as

$$P_s(t) = P_{so} \left( 1 - \frac{t}{t_o} \right) e^{-b \frac{t}{t_o}} \tag{1}$$

Where  $P_{so}$ ,  $t_o$ ,  $b$ , and  $t$  represent peak overpressure, positive phase duration, decay coefficient, and time duration.

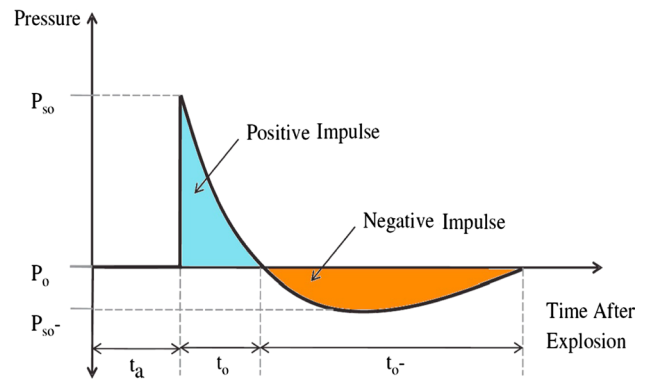
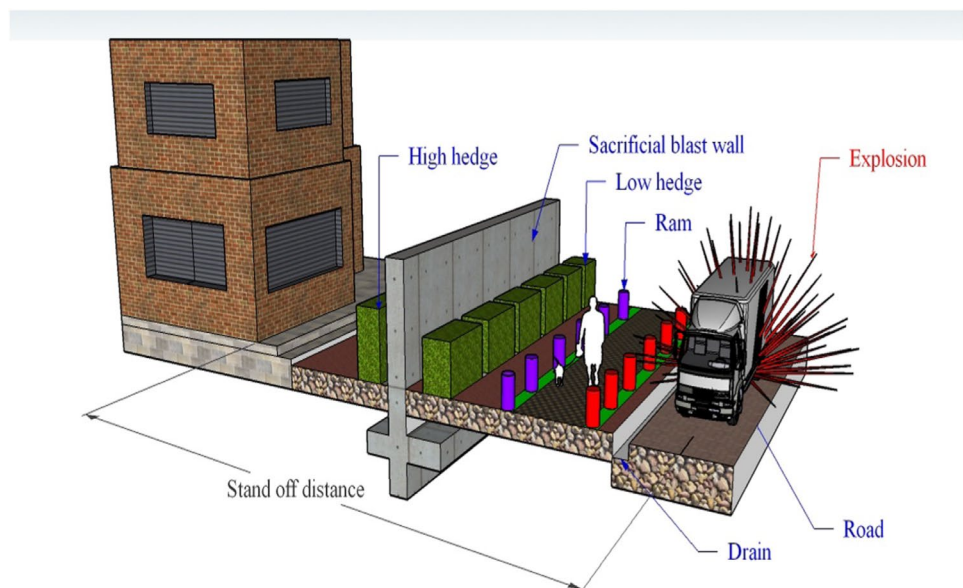


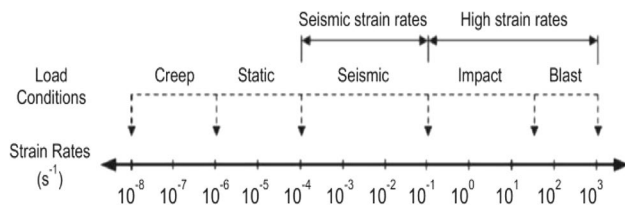
Fig. 6 Variation of pressure–time for overpressure [21]

Fig. 5 Measures to protect buildings against blast loading [20]



**Table 2** Damage by blast pressure [23]

| Damage                        | Incident overpressure (MPa × 10 <sup>-3</sup> ) | Damage   | Incident overpressure (MPa × 10 <sup>-3</sup> ) |
|-------------------------------|---|--|---|
| Breakage of window panels     | 1.03–1.52                                       | Wood framed buildings collapsed                    | > 34.48   |
| Structures with minor damages | 3.45–7.59                                       | Steel frame buildings (severely damaged)           | 27.59–41.38                                     |
| Sheet metal buckled panels    | 7.59–12.41                                      | Reinforced concrete structures (seriously damaged) | 41.38–62.07                                     |
| Concrete block walls failure  | 12.41–20  | Destroyed buildings                                | 68.96–82.76                                     |



**Fig. 7** Strain rate ranges induced by different types of loading [27]

### UHPFRC behavior under high strain rates

Under flexural loading, Millard et al. [24] examined the dynamic increase factor (DIF) of UHPFRC and plain concrete. The strain rate observed by the dynamic flexural test ranged from  $1 \times 10^{-2}$  to  $1 \times 10^1 \text{ s}^{-1}$ . The researchers found that the UHPFRC has DIFs of approximately 1.5 and 2.5 for the fiber content of 2 and 1.5%, respectively. Tedesco and Ross [25] proposed a relationship between strain rate and DIF from the modified formulation. The authors predicted the DIF for UHPFRC at a strain rate of  $1 \text{ s}^{-1}$  after the formulation. Habel and Gauvreau [5] provided the analytical and experimental analysis on UHPFRC subjected to static and low-velocity drop tests. The results showed that the UHPFRC specimen had a higher ultimate tensile strength at higher strain rates, about 25% more than the static value. Rong et al. [26] studied the dynamic behavior of ultra-high performance cement-based composites (UHPCC) and showed that the ultimate strain and peak stress of UHPCC increased with the increase in strain rates. Figure 7 illustrates different ranges of strain rates under various loading rates.

Habel and Gauvreau [5] performed direct tensile testing on UHPFRC dog bone specimens at varying strain rates ranging from  $8 \times 10^{-7}$  to  $2 \times 10^{-1} \text{ s}^{-1}$ . Maalej et al. [28] carried out the same test on engineered cementitious composites (ECC) coupons with strain rates ranging from  $2 \times 10^{-6}$  to  $2 \times 10^{-1} \text{ s}^{-1}$ . The strain rate improvement becomes more critical at higher strain rates, introducing a bi-linear DIF-strain rate equation, as described by Malvar et al. [29].

The following empirical formula is used to calculate the dynamic increase factor, provided by Comite European du Beton (CEB) model code 1990 Malvar et al. [29]

For steel reinforcement,

$$DIF = \left( \frac{\dot{\epsilon}}{10^{-4}} \right) \tag{2}$$

where

For yield strength;

$$\alpha = \alpha_{fy} - \frac{0.04f_y}{60}$$

At ultimate stress;

$$\alpha = \alpha_{fu} = 0.019 - \frac{0.009f_y}{60}$$

where  $\alpha$  coefficient is calculated by,  $f_{co} = 10 \text{ MPa} = 1450 \text{ psi}$

For concrete in compression

$$DIF = \frac{f_c}{f_{cs}} = \left( \frac{\dot{\epsilon}}{\dot{\epsilon}_s} \right)^{1.026\alpha}, \text{ for } \dot{\epsilon} \leq 30 \text{ s}^{-1} \tag{3}$$

$$DIF = \frac{f_c}{f_{cs}} = \gamma_s \left( \frac{\dot{\epsilon}}{\dot{\epsilon}_s} \right), \text{ for } \dot{\epsilon} > 30 \text{ s}^{-1} \tag{4}$$

where  $f_c, f_{cs}$  are the dynamic and static compressive strength at  $\dot{\epsilon}$ ,  $\dot{\epsilon}_s$  is the strain rate in the range of  $30 \times 10^{-6}$  to  $300 \text{ s}^{-1}$ .  $\dot{\epsilon}_s = 30 \times 10^{-6} \text{ s}^{-1}$ .

$$\log \gamma_s = 6.15\alpha_s - 2, \quad \alpha_s = \frac{1}{5 + \frac{9f_{cs}}{f_{co}}}$$

$f_{co} = 10 \text{ MPa} = 1450 \text{ psi}$

In case of concrete in tension

$$DIF = \frac{f_t}{f_{ts}} = \gamma_s \left( \frac{\dot{\epsilon}}{\dot{\epsilon}_s} \right)^{1.016\alpha}, \text{ for } \dot{\epsilon} \leq 30 \text{ s}^{-1} \tag{5}$$

$$DIF = \frac{f_t}{f_{ts}} = \beta \left( \frac{\dot{\epsilon}}{\dot{\epsilon}_s} \right), \text{ for } \dot{\epsilon} \leq 30 \text{ s}^{-1} \tag{6}$$



where  $f_t$ ,  $t_{cs}$  are the dynamic and static tensile strength at  $\dot{\epsilon}$ ,  $\epsilon$  is the strain rate in the range of  $30 \times 10^{-6}$  to  $300 \text{ s}^{-1}$ .  $\dot{\epsilon}_s = 30 \times 10^{-6} \text{ s}^{-1}$ .

$$\log \beta = 7.11\delta - 2.33, \quad \delta = \frac{1}{10 + \frac{6f_{ts}}{f_{co}}}$$

$$f_{co} = 10 \text{ MPa} = 1450 \text{ psi}$$

### Scaling laws

The scaled distance is used to evaluate blast explosions with different standoff distance weights of charge. For example, if different charge weights of the same explosive are given, similar blast waves occur at identical scaled distances. Hopkinson [30] first presented the empirical formula of scaled distance in 1915 and then referred to by Baker [31] in 1973.

$$Z = \frac{R}{W^{1/3}} \tag{7}$$

$Z$  is the scaled distance,  $R$  is the standoff distance, and  $W$  is the charge weight.

Another modified formula is given as Sachs scaling by Baker [31] in 1973. It is used for the blast when there is a change in atmospheric pressure between the source and the target. The equation is as follows.

$$\bar{R} = R \frac{P_o^{1/3}}{E^{1/3}} \tag{8}$$

where  $\bar{R}$  is the Sachs distance,  $P_o$  is the ambient pressure, and  $E$  is the energy of the explosive charge.

### Equivalent explosive weight

Using explosive devices against building structures is the most frequent target of terrorist strikes. There should be some procedure to be followed to design the structural

elements practically. The first step to designing a structure to withstand blast loading to define the type and weight of the explosive charge. Several explosives are available nowadays for conducting blasts on the structure. An improvised explosive device (IED) is a solid explosive that will be widely used in large cases. IEDs can easily be transported, ease of manufacture, and the ability to be placed in vehicles that could travel in the area, adjacent or within a structure. Trinitrotoluene (TNT) is a standard material have safe to be handle, pure, and readily available explosive. Trinitrotoluene (TNT) is the standard explosive used for assessing the effects of blast loading. The TNT is used to convert the charge mass of the explosive, which is increased by a conversion factor based on the charge's specific energy. The first step is to convert the charge weight into an equivalent mass of TNT. The unified facilities criteria (UFC 3-340-02) [32] code expresses TNT by an equation.

$$W_{EFF} = \frac{H_{Exp}^d}{H_{TNT}^d} W_{TNT} \tag{9}$$

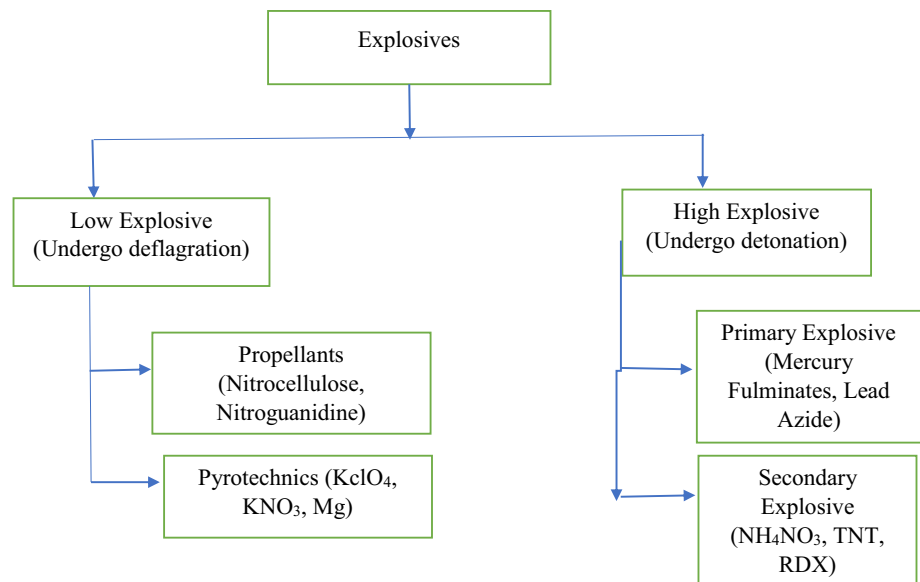
where  $W_{EFF}$  is the effective charge is the mass of TNT equivalent (kg),  $H_{Exp}^d$  is the heat of detonation (J/kg),  $W_{TNT}$  is the mass of TNT (kg), and  $H_{TNT}^d$  is the heat of detonation of TNT (kg). The explosive charge weight is measured in kg of TNT, which can be converted as shown in Table 3, and different explosives are classified as shown in Fig. 8.

Scaled distance ( $Z$ ) depends on peak static and reflected blast pressure. Scaled distance is defined as the ratio of standoff distance ( $R$ ) to the cube root of charge weight ( $W$ ). Scaled Distance,  $Z = R/W^{1/3}$ . Peak pressure  $W/R^3$  is another way to look at the scaled distance and pressure relationship. It implies that if the standoff distance is doubled, the peak pressure reduces eight times. Thus, to minimize the impact of the blast, it is vital to maintain a suitable standoff distance. The UFC (3-340-02) [32] code also gives a minimum standoff distance of 15ft for any structure to resist the effect of Blast loading. Figure 9 shows graphs for analytical results to calculate peak positive overpressure,  $P_{so}$ , and scale distance  $Z$ .

**Table 3** Factors of conversion for explosives [22]

| Explosive        | Density (kg/m <sup>3</sup> ) | TNT equivalency for pressure (kN) | TNT equivalency for impulse (kN) |
|------------------|------------------------------|-----------------------------------|----------------------------------|
| TNT              | 1630                         | 1.00                              | 1.00                             |
| Amatol           | 1590                         | 0.97                              | 0.87                             |
| Composition C4   | 1590                         | 1.20                              | 1.19                             |
| ANFO (94/6 ANFO) | 800                          | 0.87                              | 0.87                             |
| Tritonal         | 1720                         | 1.07                              | 0.96                             |
| RDX              | 1820                         | 1.10                              | 1.10                             |
| PETN             | 1770                         | 1.27                              | 1.27                             |
| HMX              | –                            | 1.25                              | 1.25                             |

**Fig. 8** Classification of explosives [33]



Determination of the blast loading depends on the horizontal distance from the ground and the location of the explosion. There are three types of blast according to location. The free air blast occurs in the air and travels directly on the building without any obstacle. Air blast is the type of explosion, which happens in the air, but the wave hits the ground before traveling on the building surface. Surface/ground blast is the type of blast, which occurs on the ground, and the wave hits the ground after then traveling on the building surface. These are illustrated in Fig. 10.

## Blast wave prediction

The ambient pressure rises and then falls during a blast, producing a triangular overpressure. Free air blast empirical formula is given in Table 4.

$Z$  is specified by:

$$Z = \frac{R}{W^{\frac{1}{3}}} \left( \text{m/kg}^{\frac{1}{3}} \right)$$

where  $Z$  is the scaled distance ( $\text{m/kg}^{1/3}$ ),  $R$  is the standoff distance (m), and  $W$  is the weight of charge (kg). Extensive charts for predicting blast durations and pressures are provided by (Department of the Army, The Navy 1990). Table 5 lists the numerical values of peak reflected overpressure with different  $W$ - $R$  combinations.

## Published literature

Much research has been done so far on blast loading, the pressure it exerts on the different components of the structure, and its impact on the structure. Here is a review of the

literature already available related to the effect of blast loading on the structure. The research work of various authors has been summarized, and appropriate conclusions have been drawn. This helps better understand the subject and helps identify the gap areas in the scholar's research. It is worth mentioning that the critical analysis of published work has been reviewed under different categories under flexural and compression members.

## Flexural members

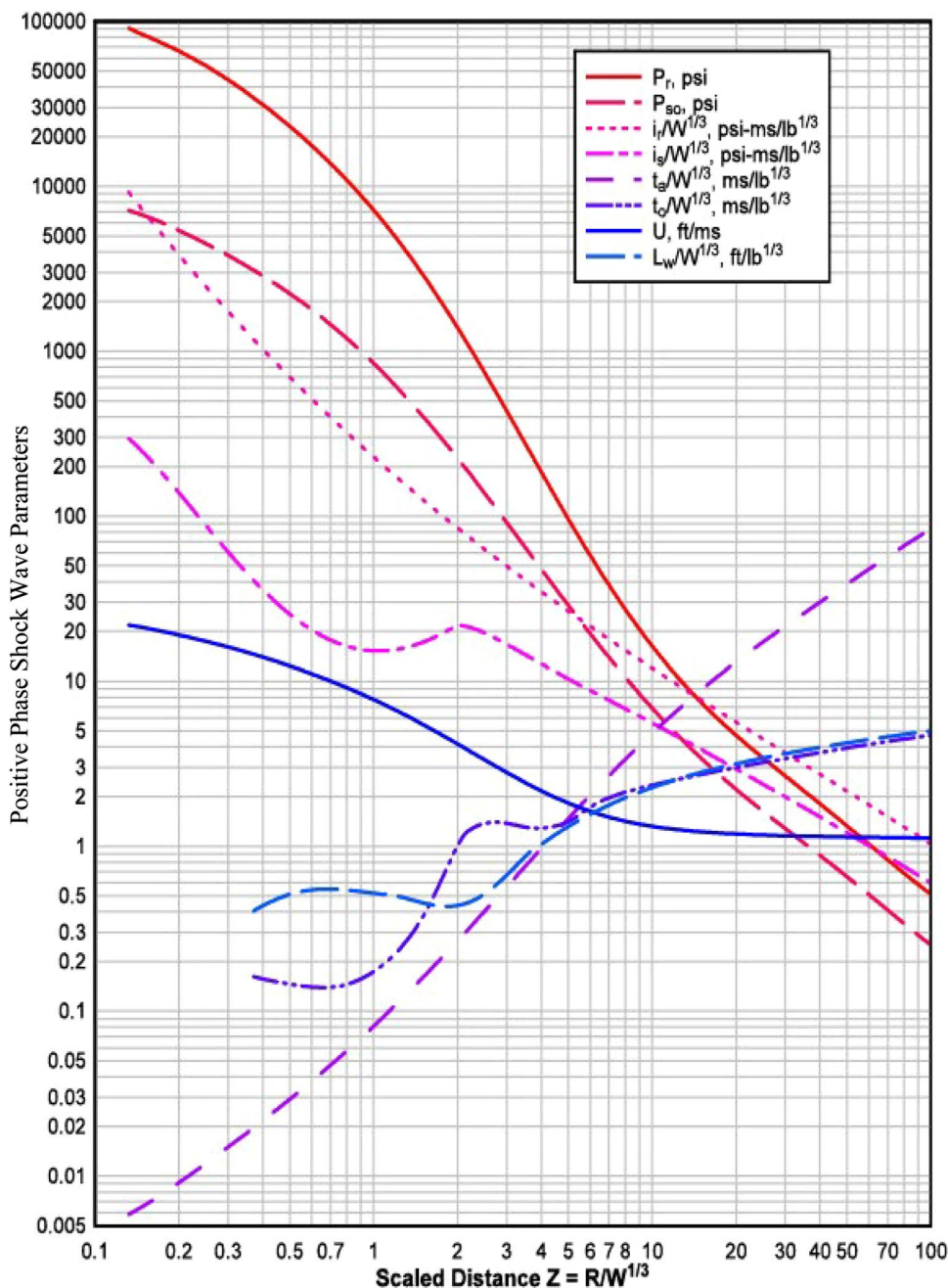
### Experimental investigations

The experimental investigations are subdivided into standoff distance, charge weight, and magnitude of charge weight.

**Based on standoff distance** Mahmud et al. [48] studied the bending behavior of 26 UHPFRC slab specimens. They tested slabs of different thicknesses under fixed and simply supported (SS) conditions. At the failure conditions, authors concluded that micro-cracks are developed at the fixed end of the slabs of 25 and 35 mm thicknesses, respectively. The authors found the load–displacement behavior of UHPFRC slabs linear, illustrating pseudo-strain hardening and strain softening. Ha et al. [49] used two-way panels made of NSC, high-strength concrete (HSC), and UHPFRC to perform close-in blast testing. The plates, which were  $1000 \times 1000 \times 150$  mm, were fastened on all sides and tested with explosive weights (ANFO) ranging from 4 to 16 kg at a standoff distance of 1.5 m. UHPFRC plates had better blast performance, less residual displacement, and less cracking than NSC and HSC plates. The results showed that the RC panels retrofitted with polyurea (PU), carbon fiber-reinforced polymer (CFRP), or hybrid fibers possess



**Fig. 9** Blast wave characteristics for a hemispheric TNT explosion at sea level on the surface UFC 3-340-02 [32]



significantly higher stiffness and ductility to withstand blast loads when compared with those of NSC. Wu et al. [1] performed several tests to investigate UHPFRC slabs  $2000 \times 1000 \times 100$  mm with and without reinforcement and then retrofitted with fiber-reinforced polymer (FRP). When tested under blast loads, the results indicated that the UHPFRC slab has more minor damage than NRC slabs.

**Based on magnitude of charge weight** Schleyer et al. [50] conducted full-size explosive testing of fiber-reinforced concrete (FRC) panels. The panels were held inside a large concrete cover to prevent the effect of blast on the surroundings

and only subject the panels to the blast load. 100 kg TNT explosive charges were placed at various distances between 12 and 7 m. Of the four panels constructed, two were built with multiple levels of steel fibers quantity. The other two panels were made using steel fiber and supplementary steel bar reinforcement. They concluded that the four UHPFRC panels were subjected to blast loads from the 100 kg TNT charge weight, and then panels were analyzed after the blast.

**Based on characteristics strength** Several investigators studied the dynamic constitutive model for UHPFRC, Du et al. [51]. According to the Holmquist–Johnson–Cook

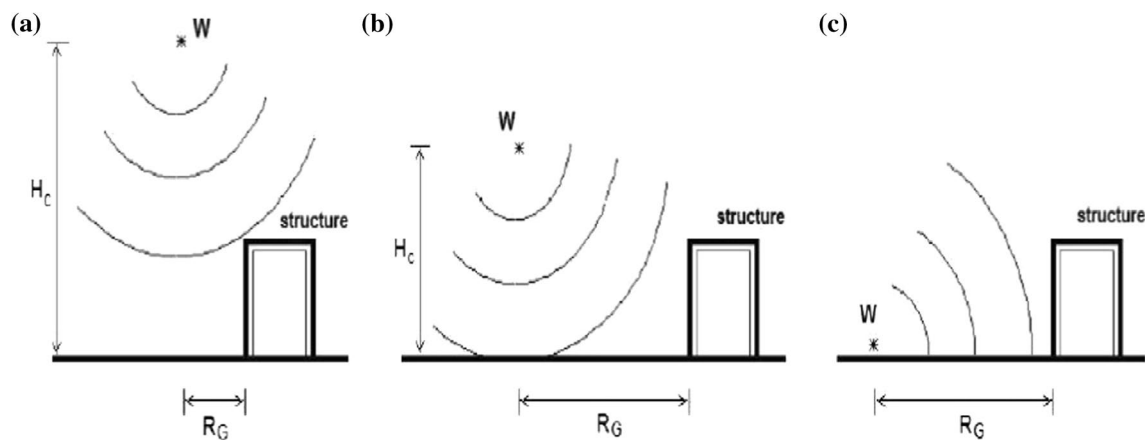


Fig. 10 Types of blast loading: (a) free air blasts, (b) air blasts, and (c) surface blasts (Karlos and Solomos [22])

Table 4 Empirical models for the peak positive overpressure

| S. No | Empirical model                             | Equations   |
|-------|---|---|
| 1     | Brode [34]                                  | $P_{so} = \frac{0.0975}{Z} + \frac{0.1455}{Z^2} + \frac{0.585}{Z^3} - 0.0019, (0.01 < P_{so} < 1)$  |
| 2     | Henrych and Major [35]                      | $P_{so} = \frac{0.67}{Z^3} + 1$ for $(P_{so} > 1)$<br>$P_{so} = \frac{1.4072}{Z} + \frac{0.5540}{Z^2} - \frac{0.0357}{Z^3} + \frac{0.000625}{Z^4}$ , for $(0.05 < Z < 0.3)$<br>$P_{so} = \frac{0.6194}{Z} - \frac{0.0326}{Z^2} + \frac{0.2132}{Z^3}$ , for $(0.3 < Z < 1)$<br>$P_{so} = \frac{0.0662}{Z} + \frac{0.405}{Z^2} + \frac{0.3228}{Z^3}$ , for $(1 < Z < 10)$ |
| 3     | Held [36]                                   | $P_{so} = \frac{2}{Z^2}$ MPa  |
| 4     | Mills [37]                                  | $P_{so} = \frac{0.108}{Z} - \frac{0.114}{Z^2} + \frac{1.772}{Z^3}$  |
| 5     | Sadovskiy [38]                              | $P_{so} = \frac{0.085}{Z} + \frac{0.3}{Z^2} + \frac{0.8}{Z^3}$  |
| 6     | Bajic [39]                                  | $P_{so} = \frac{0.102}{Z} + \frac{0.436}{Z^2} + \frac{1.4}{Z^3}$  |
| 7     | Kinney and Graham [40]                      | $P_{so} = P_o \cdot \frac{80.8 \left[ 1 + \left( \frac{Z}{4.5} \right)^2 \right]}{\sqrt{\left[ 1 + \left( \frac{Z}{0.048} \right)^2 \right] \times \left[ 1 + \left( \frac{Z}{0.32} \right)^2 \right] \times \left[ 1 + \left( \frac{Z}{1.35} \right)^2 \right]}}$  |
| 8     | TM 5-855-1 [41]                             | $P = \frac{39.5}{Z} - \frac{105}{Z^2} + \frac{4120}{Z^3}$ for $(2 < P < 160), (3 < Z < 20)$   |
| 9     | Newmark and Hansen (for surface blast) [42] | $P_{so} = \frac{0.6784}{Z^3} + \frac{0.294}{Z^{\frac{3}{2}}}$   |
| 10    | Wu and Hao (surface blast) [43]             | $P_{so} = 1.059 \times Z^{-2.56} - 0.051$ , for $(0.1 \leq Z \leq 1)$<br>$P_{so} = 1.008 \times Z^{-2.01}$ , for $(1 < Z \leq 10)$  |
| 11    | Siddiqui and Ahmad (surface blast) [44]     | $P_{so} = 1.017 \times Z^{-1.91}$ , for $(1 \leq Z \leq 12)$  |
| 12    | Ahmad et al. (surface blast) [45]           | $P_{so} = 2.46 \times Z^{-2.67}$  |
| 13    | Iqbal and Ahmad (surface blast) [46]        | $P_{so} = 1.026 \times Z^{-1.96}$ , for $(1 \leq Z \leq 12)$  |

Table 5 Peak reflection pressure  $P_r$  (MPa) with different  $W$ - $R$  combination Ngo et al. [47]

| $W$ (Kg TNT) ↓ | $R$ (m) → |       |       |      |      |      |      |      |
|----------------|-----------|-------|-------|------|------|------|------|------|
|                | 1         | 2.5   | 5     | 10   | 15   | 20   | 25   | 30   |
| 100            | 165.8     | 34.2  | 6.65  | 0.8  | 0.27 | 0.14 | 0.09 | 0.06 |
| 500            | 345.5     | 89.4  | 24.8  | 4.25 | 1.25 | 0.54 | 0.29 | 0.19 |
| 100            | 464.5     | 130.8 | 39.5  | 8.15 | 2.53 | 1.06 | 0.55 | 0.33 |
| 2000           | 602.9     | 188.4 | 60.19 | 14.7 | 5.01 | 2.13 | 1.08 | 0.63 |

model (HJC model), the addition of steel fibers caused two changes: a change in yield surface and a change in strain range effect. Several mechanical tests of UHPFRC, such as uniaxial bending, compression, and uniaxial cyclic loading, were carried out to examine the model parameters. The simulation results found that the stress–strain curves and failure morphology were better when the erosion strain was 1.0%. Banerji et al. [52] experimented with the behavior of UHPFRC beams subjected to extreme loading effects on structures and fire conditions. Five beams were tested to calculate the behavior of the structure and spalling performance under fire conditions. The test results showed that due to the inclusion of polypropylene fiber in UHPFRC beams, fire resistance increases significantly when compared with NSC. It was concluded that the UHPFRC beams are more susceptible to fire due to spalling than normal concrete. The addition of propylene fibers in UHPFRC beams enhanced fire resistance. Astarlioglu and Krauthammer [53] investigated the blast resistance of columns using one degree of freedom (ODOF) analysis, boundary conditions, and axial loads. It was observed that the UHPFRC columns were damaged 27–30% less than NSC columns with supported ends. Similarly, in the case of impulse loading, the UHPFRC compression columns can continue to take 400% additional load than the impulse, causing the NSC columns to break. The NSC and UHPFRC displayed diverse behavior when quasi-static stresses were applied. The reflected pressure values for quasi-static loads represented by a horizontal asymptote on the impulsive load diagram in the case of NSC were generally the same as for fixed and supported end conditions, respectively. Ellis et al. [54] conducted experiments on UHPFRC panels of  $1626 \times 864 \times 51$  mm without steel reinforcement under blast loading. The authors concluded that packing, fiber geometry, and volume enhance tremendously the resistance of UHPFRC structures subjected to blast loading. Yi et al. [27] present the behavior and properties of UHPC and RPC subjected to blast load. The behavior of UHPC and RPC was studied using flexural strength, elastic modulus, compressive strength, and slump flow test. They showed that UHPC and RPC are more resistant to blast explosions than NSC. Barnett et al. [55] cast a series of panels UHPFRC  $3500 \times 1300 \times 100$  mm subjected to 100 kg of TNT under blast loading. The variables included in this research were type and quantity of fiber reinforcement and standoff distance. The results concluded that the UHPFRC had improved properties against explosions. Cavili and Rebstrost [56] performed several blast tests on different panels cast with RPC. RPC is a UHPFRC material made of cement, silica flour, silica fume, sand, steel fibers and water, and a superplasticizer. The composite material pos-

sesses compressive strength in 160–200 MPa, while the flexural strength is 30–40 MPa.

Numerous experimental studies have been conducted to examine performance of UHPFRC subjected to impact loading. However, very few investigations have been published on studies pertaining to performance of this noble material when subjected to blast loads probably because of obvious reasons of limited and exorbitantly expensive testing facilities, restrictions on use of explosives due to security reasons, strategic importance of research, non-availability of patented research publications, etc. Non-availability of quality research papers due to heavy payment, defense agencies, and costly instrumentation, measuring devices, sensors, data acquisition systems, software, etc., other major constraints which are observed as a major obstruction in research and development in the domain of studies on blast-resistant structures.

Threat of terrorist attacks using explosives has greatly heightened the awareness among the architects, designers and owners, and private sector is considering measures to structures that are vulnerable to collateral damage. Govt. agencies are funding research in design and analysis of blast resistant. The critical review of experimental studies conducted by various researchers illustrated that the blast loading is becoming more popular in the field of structural engineering. The experiment studies were conducted considering influence of different parameters such as standoff distances, charge weights, type of blast loading (surface, air blast, etc.), and strength of composites. The critical analysis of experimental study conducted by various researchers indicated that several researchers conducted studies on RC, HPC and HSC structures when they are subjected to blast loads. However, research considering material and structural nonlinearities is missing. Very few studies on UHPFRC structures subjected to blast loads are conducted considering limited variables using material properties. Research on UHPFRC structure is either very limited or non-existent. The present study is very useful for the analysis and design of structures against high-strain-rate loading effects.

### Analytical investigation

**Based on charge weight** Castedo et al. [57] investigated the response of three reinforced concrete (RC) slabs against blast loading at the close in detonation with full-scale testing and simulation. Both the slabs were exposed at charge weights of 1.74 and 13.05 kg of TNT at a 1 m. The slab with blast loading was described using the finite model with load blast enhanced (LBE) tool. It was observed that the LBE model has better test results regarding the perforation of the slab.

**Based on strength of concrete** Kadhim et al. [58] investigated the durability and mechanical properties of UHPC material. UHPC is more costly than normal concrete (NC) and offers superior compressive and cracking tensile strength. The authors developed a finite element (FE) model that accurately depicts the behavior of UHPC beams with and without fibers. It was found that when the thickness of the hybrid increases, UHPC-NC beams with top and bottom layers rise, and the load-carrying capacity increases. Almustafa and Nehdi [59] investigated using the machine-learning model to determine the extreme displacement of RC slabs when subjected to blast loading. They concluded a database of 150 points was compiled. The influence of slab length, width, thickness, compressive strength, reinforcing bar strength, steel reinforcing ratio, reflected impulse, blast scale distance, slab type, and slab support was considered. The machine-learning model performed well in expecting extreme displacements of RC slabs subjected to blast loading when these data were verified. Elvira et al. [60] compared some of the available research methods for progressive collapse of structural design, ranging from simple linear static analysis to the most complex and time-consuming nonlinear dynamic analysis, which considers both the primary and secondary effects of blast loading. However, because of the non-availability of any blast loading code, there is no standard procedure for analyzing structures that have been exposed to blast loading. It was concluded that when the charge weight was at 5 m, the response on the floor behaved accurately. Table 6 provides the details experimental and analytical studies of flexural members on the basis of sample size, charge weights, explosive types, and the material. The critical review of analytical studies conducted by various researchers is available using different FE software like CONWEP, LS-DYNA, AUTODYN, ABAQUS, ANSYS, Air3D, and 3D Blast), for modeling the structure subjected to blast loading. Various design codes are available for the blast loading such as US Department of Defense (DOD), Federal Emergency Management Agency (FEMA), American Society of Civil Engineers (ASCE), American Concrete Institute (ACI), NCHRP Report 645 (2010), and IS 4991 (1968), etc.

## Compression members

### Experimental investigations

Lee et al. [109] examined the influence of blast and impact resistance of 6 RC columns which were designed and detailed for seismic conditions. Shock-tube and drop weight tests were used to test the columns of size  $160 \times 160 \times 2468$  mm. The blast effects and impact resistance of columns improved, thanks to UHPFRC and seismic detailing. They concluded that the use of UHPFRC jacketed

columns subjected to blast loading have maximum and residual displacements. Table 6 illustrates the classification of different elements, sample size, different charge weights, their standoff distances, and material properties.

### Analytical investigations

UHPFRC is a recent cement-based material with compressive strength higher than 150 MPa and improved extreme flexural and tensile strengths, durability, and ductility, according to Shaikh et al. [110]. UHPFRC mixture was determined by adding 2–3% of high steel fibers and a low water–cement ratio  $< 0.2$ . UHPFRC were obtained under curing at 90 degrees. The UHPFRC material has 2.2 times higher compressive and tensile strength than ordinary concrete. Zhang et al. [21] investigated the failure behavior and response of RC members subjected to blast loading. Typically, RC structures demonstrated brittle behavior and spalling due to extreme rate explosions. The researchers adopted different finite element (FE) techniques for the simulation of blast loading. The response and failure behavior of RC structures were then studied. Buttignol et al. [111] give an extensive review of the properties of UHPFRC and the developments in the design procedures for UHPFRC. UHPFRC has exceptional properties like high ductility, low permeability, extraordinary compressive strength, and high toughness compared to conventional concrete. However, there are no specific design codes for UHPFRC as it is new material. The improved properties of UHPFRC are hydration process, permeability, the role of fibers, mix design, workability, and curing. The mechanical properties of UHPFRC include flexural and tensile strength, size effect, creep, shrinkage, tensile strength, shear and punching, and shear properties. The authors found that, in UHPFRC mixes, incorporating binding materials of more than  $1000 \text{ kg/m}^3$  enhances production cost and mixing procedures. An optimization of binding material is therefore essential to decrease quantity of binding material without weakening the UHPFRC composite.

Remennikov and Carolan [112] elaborated on the blast loading and its impact on various structures. Air blasts and surface blasts are also explained based on TM-500 (US Army, 1991) [41]. The different types of pressure that incident on the structure, i.e., reflected pressure, incident pressure, and dynamic pressure, are also discussed. They introduced different concepts that can be adopted in mitigating the terrorist threats. The methods for improving protection of structure by adopting relatively economical measures of design were also suggested. Dragani and Sigmund [113] studied the blast loading effect on the structure analytically. A fictitious structure was taken to determine the pressure time history with the help of SAP2000 software. Their results showed that at each point, the ductility is

**Table 6** Experimental and analytical investigations by different researchers on flexural members

| S. No | Researchers                | Elements   | No. of specimens | Sample size (m)               | Charge wt. (kg)/explosive/standoff distance (m) | Material               | Type of testing             | Properties studied  |
|-------|----------------------------|------------|------------------|-------------------------------|---|------------------------|-----------------------------|---|
| 1     | LOK and XIAO [61]          | Panel      | 42               | –                             | 8,20,30,40/PETN/5                               | SFRC                   | Experimental                | Residual displacement                                     |
| 2     | Mays and Hetherington [62] | Wall panel | 7                | –                             | 110,150,155,165, 195/PE4/0.8,1,2                | RC                     | Experimental                | Crack pattern   |
| 3     | Lan et al. [63]            | Beam       | 32               | –                             | 8–100/TNT/5                                     | RC, PSSRC, SFRC, SASS, | Experimental                | Airblast overpressure, acceleration, maximum displacement |
| 4     | Hoemann et al. [64]        | Wall panel | 8                | –                             | –/11/–  | FRP                    | Experimental                | Blast fragmentation                                       |
| 5     | Ngo et al. [65]            | Panel      | 4                | 2×1×0.40                      | 6000/TNT/30,40                                  | UNSC, NSC              | Experimental                | Crack pattern   |
| 6     | Ohtsu et al. [66]          | Slab       | 4                | 0.6×0.6×0.1                   | 0.01/Dynamite/–                                 | RC, FRC, PVAFRC, PPFRC | Experimental and Analytical | Spalling, Crack   |
| 7     | Ghani Razaqpur et al. [67] | Panel      | 8                | 1×1×0.07                      | 22.4,33.4/ANFO/3                                | GFRP                   | Experimental                | Post blast damage, mode of failure                        |
| 8     | Silva and Lu [68]          | Slab       | 5                | 1.2×1.2×0.09                  | 0.45,0.9,1.35/RDX/0.3,0.91                      | RC                     | Experimental                | Blast resistance capacity, displacement                   |
| 9     | Schenker et al. [69]       | Slabs      | 4                | 1×1×1.5                       | 1000/TNT/1                                      | RC                     | Experimental and Analytical | Dynamic response  |
| 10    | Zhou et al. [70]           | Slab       | 4                | 1×1.3×0.1                     | 0.5/ANFO,RDX, TNT/0.1                           | RC, HSSFC              | Experimental and Analytical | Dynamic plastic damage model                              |
| 11    | Wu et al. [71]             | Slab       | 6                | 1.3×1×0.12                    | 2.1/TNT/0.6                                     | RC, CFRP               | Experimental                | Deflection, Pressure                                      |
| 12    | Wu et al. [1]              | Slab       | 2                | 2×1×0.1                       | 1,3,4,8/–/0.75,0.92,1,1.4,1.5,3                 | FRP                    | Experimental                | Fragmentation   |
| 13    | Beppu et al. [72]          | Slab       | 14               | 0.5×0.5×0.08                  | –/C4/–  | FRP                    | Experimental                | Local damage, fragmentation                               |
| 14    | Urgessa and Maji [73]      | Wall panel | 8                | 1.02×3.05×0.203               | 1.09/TNT/–                                      | FRP                    | Experimental                | Displacement, Stiffness failure pattern                   |
| 15    | Yusof and Norazman [74]    | Panels     | 4                | 0.6×0.6×0.1                   | 1/TNT/0.6                                       | SFRC                   | Experimental                | Cracks  |
| 16    | Garfield et al. [75]       | Wall panel | 18               | 1.2×1.2×(0.152, 0.254, 0.356) | 6.1,12.8/C4, ANFO/1                             | NWC, FRC, GFRP         | Experimental and analytical | Crack pattern   |
| 17    | Ha et al. [49]             | Panel      | 9                | 1×1×1.5                       | 15.88/ANFO/1.5                                  | CFRP                   | Experimental                | Blast-resistant capacity, residual displacement           |
| 18    | Morales-Alonso et al. [76] | Slab       | 12               | 0.5×0.5×0.08                  | 3,4/TNT/1.5                                     | RC                     | Experimental and analytical | Cracking pattern, deflection                              |
| 19    | Wu et al. [77]             | Slab       | 5                | 2×1×0.1                       | 8,14/COMP B/0.92,1.47,1.5                       | RC                     | Experimental                | Acceleration, Deflection                                  |



**Table 6** (continued)

| S. No | Researchers            | Elements | No. of specimens | Sample size (m) | Charge wt. (kg)/explosive/standoff distance (m) | Material          | Type of testing             | Properties studied                              |
|-------|------------------------|----------|------------------|-----------------|---|-------------------|-----------------------------|---|
| 20    | Yamaguchi et al. [78]  | Slab     | 13               | 0.6×0.6×0.05    | 0.2/Penthrith, paraffin/0.06                    | RC, PEFRC         | Experimental and analytical | Spall damage                                    |
| 21    | Yi et al. [27]         | Beam     | 6                | 1×1×0.15        | 4.08,15.88/TNT/1.5                              | NSC, UHSC, RPC    | Experimental                | Residual displacement, blast-resistant capacity |
| 22    | Foglar and Kovar [79]  | Slab     | 5                | 1.2×1.2×0.9     | 25/TNT/4  | FRC               | Experimental and analytical | Spalling, deflection                            |
| 23    | Tabatabaei et al. [80] | Panel    | 7                | 1.83×1.83×0.13  | 38.5/<br>ANFO/1.065,1.375,1.675                 | RC, LCFRC         | Experimental and analytical | Damage, cracking, spalling                      |
| 24    | Chen et al. [81]       | Wall     | 4                | 1.5×2×0.2       | 0.2,3,9,21,2,30,34.2/<br>TNT/5.86               | CFRP              | Experimental and analytical | Failure mode, fragmentation                     |
| 25    | Mao et al. [82]        | Panel    | 4                | 3.5×1.3×0.1     | 100/TNT/7,9,12                                  | UHPFRC            | Experimental and analytical | Strain rate                                     |
| 26    | Orton et al. [83]      | Slab     | 4                | –               | –   | CFRP              | Experimental                | Blast resistance, deflection                    |
| 27    | Castedo et al. [84]    | Slab     | 8                | 4.46×1.46×0.15  | 2,15/TNT/0.5,1                                  | RC                | Experimental and analytical | Damage pattern, plastic strain                  |
| 28    | Foglar et al. [85]     | Slab     | 6                | 6×1.5×0.3       | 25/TNT/3  | RC                | Experimental and analytical | Concrete spalling, breach prediction curves     |
| 29    | Li et al. [8]          | Slab     | 5                | 2×1×0.1         | 1–14/TNT/1–7.35                                 | NSC, UHPC         | Experimental and analytical | Time history, flexural damage                   |
| 30    | Li et al. [86]         | Slab     | 2                | 2×0.1×0.1       | 1/TNT/0   | NSC, UHPC         | Experimental and analytical | Time history curves                             |
| 31    | Alengaram et al. [87]  | Slab     | 7                | 2×1×0.2         | 1,5,10/TNT/1.5                                  | OPSC, OPS-FRC     | Experimental                | Ductility behavior, cracks                      |
| 32    | Alsayed et al. [88]    | Panel    | 6                | 3.5×2.4×0.4     | 1.134,14.2,49.9/C4/2,4.8                        | GFRP              | Experimental & analytical   | Debonding failure, the damage pattern           |
| 33    | Li et al. [89]         | Slab     | 5                | 2×0.8×0.12      | 6,12/TNT/1.5                                    | HPC               | Experimental                | Dynamic performance, structural damage          |
| 34    | Li et al. [90]         | Slab     | 7                | 2×0.8×0.1       | 0.1,1/TNT/0                                     | NRC, UHPC         | Experimental                | Crater diameter, spall damage                   |
| 35    | Oña et al. [91]        | Slab     | 16               | 0.5×0.5×0.05    | 3.33,4.57/TNT/1.5                               | RC, SFRC, PFRC    | Experimental and analytical | Strain rate                                     |
| 36    | Xia et al. [92]        | Slab     | 6                | 2×0.8×0.12      | 8/TNT/1.5                                       | Foam Protected RC | Experimental                | Energy absorption capacity, blast mitigation    |



**Table 6** (continued)

| S. No | Researchers          | Elements | No. of specimens | Sample size (m) | Charge wt. (kg)/explosive/standoff distance (m) | Material              | Type of testing             | Properties studied                      |
|-------|----------------------|----------|------------------|-----------------|---|-----------------------|-----------------------------|---|
| 37    | Zhai et al. [93]     | Beam     | 5                | 2.5×2.5×0.2     | 7/TNT/1.5                                       | RC                    | Experimental                | Dynamic response, crack                 |
| 38    | Bibora et al. [94]   | Beam     | 3                | 0.5×0.5×0.04    | 0.15/SEMTEX 10/0.1                              | UHPC                  | Experimental                | Dynamic deflection                      |
| 39    | Foglar et al. [95]   | Slab     | 6                | 6×1.5×0.3       | 25/TNT/0.45                                     | HPFRC, UHPFRC         | Experimental and analytical | Spalling, blast damage                  |
| 40    | Li et al. [96]       | Panel    | 10               | 3×2×2           | –/–/40  | AAC                   | Experimental                | Damage modes, the failure process       |
| 41    | Luccioni et al. [97] | Slab     | 9                | 0.55×0.55×0.05  | 0.049,0.244,0.488/TNT/0.0183,0.244, 0.276       | HSFRC                 | Experimental                | Flexure response, fracture energy       |
| 42    | Wang et al. [98]     | Panel    | 6                | 3.6×2.8×0.36    | 2.5,8,20/TNT/1,3,10                             | Unreinforced concrete | Experimental                | Failure mode, crack                     |
| 43    | Wu and Li [99]       | Slab     | 8                | 2×0.8×0.12      | 6,12/TNT/1.5                                    | RC                    | Experimental                | Energy absorption capacity, deformation |
| 44    | Choi et al. [100]    | Slab     | 3                | 1.4×1×0.3       | 25/ANFO/–                                       | RC, PSC, PSRC         | Experimental                | Reflected pressure, impulse             |
| 45    | Hajek et al. [101]   | Slab     | 3                | 1.83×1.83×0.165 | 34/TNT/0.45                                     | RC                    | Experimental                | Damage                                  |
| 46    | Liao et al. [102]    | Beam     | 2                | 1.7×0.15×0.3    | –/–/–   | RC                    | Analytical                  | Dynamic response, resistance curve      |
| 47    | Peng et al. [103]    | Slab     | 4                | 2×0.8×0.12      | 0.05,0.1,0.2,0.4,0.6, 0.8,1/TNT/–               | UHP-SFRC              | Analytical                  | Crater depth                            |
| 48    | Zhao et al. [104]    | Slab     | 3                | 1×1×0.075       | 0.4/TNT/–                                       | RC, SSSC, CSC         | Experimental and analytical | Damage pattern                          |
| 49    | Yang et al. [105]    | Slab     | 11               | 2×2×0.1         | 2.3,3.4,5.6/TNT/0.5                             | NC, RC                | Experimental and analytical | Deflection, failure mode                |
| 50    | Junwu et al. [106]   | Slab     | 4                | 1×1×0.04        | 0.2–0.55/TNT/0.4                                | RC                    | Experimental & analytical   | Damage contour, dynamic response        |
| 51    | Kumar et al. [107]   | Slab     | 6                | 1×1×0.1         | 0.2–0.46/TNT/100,500                            | RC                    | Experimental and analytical | Failure modes                           |
| 52    | Li et al. [108]      | Slab     | 3                | 1×1×0.04        | 0.85/TNT/1.6,3,3.5                              | RC                    | Experimental and analytical | Dynamic response                        |

RC Reinforced concrete, NSC Normal strength concrete, NWC Normal weight concrete, SFRC Steel fiber-reinforced concrete, PSSRC Profile steel sheeting reinforced concrete, SFRC Steel fiber-reinforced concrete, SASS Steel air steel sandwich, SCSS Steel concrete steel sandwich, FRP Fiber-reinforced polymer, UHSC Ultra high strength concrete, FRC Fiber-reinforced concrete, PVAFRC Polyvinyl alcoholic fiber-reinforced concrete, PPFRC Polypropylene fiber-reinforced concrete, GFRP Glass fiber-reinforced polymer, HSSRC High strength steel fiber concrete, CFRP Carbon fiber-reinforced polymer, PEFRC Polyethylene fiber-reinforced concrete, LCFRC Long carbon fiber-reinforced concrete

satisfied and the deformation behavior were also checked. Hao et al. [114] studied the performance of RC columns with or without fiber-reinforced plastic (FRP) to resist blast loads. The pressure impulse (*P–I*) curve showed

damage based on axial capacity with or without FRP or both. The author demonstrated that the use of FRP on RC columns leads to carrying effective blast loads.

Table 7 summarizes the experimental and analytical studies of compression members on the basis of sample size, charge weights, explosive types, and the material.

An extensive review of published literature conducted on numerical and experimental studies illustrated that the investigations have been made on OSC, HSC, and HPC

**Table 7** Experimental and analytical investigations by various researchers on compression members

| S. No | Researchers/elements              | Sample size (m)/charge wt (kg)/explosives/standoff distance (m)     | Material     | Major conclusions/remarks   |
|-------|-----------------------------------|---|--------------|---|
| 1     | Fujikura et al. [115]/Column      | Rectangular size = 0.4 × 0.125/–/–/–                                | CFST         | CFST columns exhibit improved ductile performance under blast loading<br>Concrete-filled steel tubes (CFST) columns were more effective in seismic and blast resistance   |
| 2     | Fujikura and Bruneau [116]/Column | –/–/–   | RC           | Seismically designed RC column and steel jacket/retrofitted RC column showed no ductility under blast loading<br>Failure of columns by direct shear at their base rather than by flexural yielding  |
| 3     | Wu et al. [117]/Column            | Square size = .45, 0.60/25/TNT/0.9                                  | RC           | The response of composite column under blast loading was simulated using explicit dynamics and LS-DYNA software   |
| 4     | Fujikake and Aemlaor [118]/Column | Square size = 0.18/0.005, 0.013, 0.0195/ C4/–                       | RC           | Shear reinforcement in the column were found to improve residual resistance after the blast   |
| 5     | Roller et al. [119]/Column        | Circular $d = 0.5$ /–/PETN/0.667                                    | RC           | In contact blast, residual load capacity were increased by 70% in the case of retrofitted columns   |
| 6     | Codina et al. [120]/Column        | Square size = 0.23/1/TNT/15   | RC           | With the inclusion of steel jacket in RC column, the deflection was expected to decrease by 60%   |
| 7     | Fouché et al. [121]/Column        | –/–   | RC           | Seismically retrofitted RC columns using steel jackets were susceptible to direct shear failure   |
| 8     | Xu et al. [12]/Column             | Square size = 0.2/1, 8, 17.5, 35/TNT/1.5                            | UHPFRC, HSRC | UHPFRC specimens resist more shock waves and overpressure due to blast loads<br>The results showed that UHPFRC and HSRC specimens can resist shock waves and overpressure subjected to blast loading  |
| 9     | Zhang et al. [122]/Column         | Square size = 0.21/17.2, 35, 50/TNT/1.5                             | UPSC/CFDST   | Concrete-filled double skin tubes (CFDST) columns bear more blast loads w.r.t normal strength concrete<br>The axial load capacities of undamaged circular and square CFDST specimens were very similar, which were 4000 and 4025 kN, respectively |
| 10    | Li et al. [123]/Column            | Square size = 0.2/8, 17.5, 25, 35/TNT/1.5                           | UHPC         | Ultra-high-performance concrete (UHPC) columns possess greater blast-resistant capacity and performance   |
| 11    | Yuan et al. [124]/Column          | Square, size = 0.4/1/TNT/–  | RC           | Square columns showed severe damage in comparison to circular column  |
| 12    | Codina et al. [125]/Column        | Square, size = 0.23/8/TNT/0.6                                       | RC           | Steel jacketing have an excellent influence in terms of damage and deflection which are decreased up to 60%   |
| 13    | Li et al. [126]/Column            | Circular, dia = 0.325/1.06/TNT/–                                    | CFDST        | CFDST column system prevents concrete spall damage  |
| 14    | Rajkumar et al. [127]/Column      | Square, size = 0.085/8/TNT/1.5                                      | RC           | The results showed that using circular RC columns reduced blast loads than hexagonal, square, and octagonal RC columns  |
| 15    | Wang et al. [128]/Column          | Square size = 0.4/10/TNT/0.25, 0.375, 0.5, 0.75, 1.0, 1.5, 2.0, 3.0 | UHPFRC       | The displacement response of RC columns were reduced by 24% using UHPFRC protective layer   |

CFST concrete-filled steel tube, RC reinforced concrete, HSRC High-strength reinforced concrete, UHPC Ultra-high-performance concrete, CFDST Concrete-filled double skin tubes

incorporating different types of fibers on flexural and compression elements like beams, columns, slabs, etc. under below ground, on the ground and above ground conditions of blast loading. Few investigations have also been conducted on UHPFRC structural elements to study behavior under blast loading. The parameters, including the influence of standoff distance, the magnitude of charge weight, type and nature of blast loading, and strength variation, were studied on OSC, HPC, and HSC. The researchers, however, did not investigate the influence of the magnitude of charge weight, blast loading type, standoff distance, and strength of UHPFRC elements.

The aim of analysis and design of structures against the impulsive loading of blast and impact is to prevent the building due to collapse and damages that occur to cause human loss and harm to the structures. In the present review study, an integrated approach has been adopted to learn a lesson from the past research that construction be blast-resistant as there is a possibility of extensive damage due to explosions.

It is worth mentioning that UHPFRC, being very strong against high strain rates, as compared to OSC, HSC, and HPC, design of structures of strategic significance subjected to blast loading be made by adopting UHPFRC. Therefore, a better understanding of the response of the mechanical behavior of UHPFRC is essential so that structures' blast resistance design can be foolproof. Numerous questions remained unanswered about blast loading phenomenon, crater mechanism, failure mechanism and design philosophy of UHPFRC, etc., which require extensive numerical and experimental study viz-a-viz-standard codes and standards. Although the effect of fiber reinforcement, type, geometry, and percentage on the strain rate and mechanical behavior of UHPFRC under blast loading is still undiscovered and not fully understood, the composite is of paramount significance to many researchers related to military structures of strategic importance. Guidelines for preventing the progressive collapse of strategic structures need to be introduced in design standards to achieve improved blast-resistant structures. Structural detailing of UHPFRC elements under seismic loading may also offer improved performance under blast loading because the dynamic impact factor (DIF) and strain rate behavior is insignificant. Therefore, UHPFRC is considered a good composite for its blast-resistant structures application as it bearded higher than 400% of the force for almost similar reinforcement and specimen size. UHPFRCs may therefore be utilized to economize blast-resistant structures because of decreased thickness/depth of structural elements. In case of minimum thickness requirement of any structural element because of codal provisions or otherwise, UHPFRC may also be utilized to increase column free space economically.

Based on an exhaustive literature review, it may be inferred that UHPFRC possesses enhanced capacity to

disseminate a higher amount of impact favorably and blast energy and demonstrate improved behavior under damage compared to OSC, HSC, and HPC. UHPFRC has been found advantageous for its application in the case of security-related structures. Shear failure has also been observed as one of the predominant modes of failure in UHPFRC at close standoff blast loading. The addition of high strength fibers can further change failure pattern, blast response, and type of damage as low strength and low ductility fibers, when added to UHPFRC, it showed insignificant improvement in fracture energy absorption and blast performance of structures. A decrease in the diameter of fibers further increases the sensitivity rate of straight fibers. The typical observations and critical analysis have been used advantageously to identify the research gaps in the present published work to carry forward the research in the area.

## Summary and conclusions

Explosion near or around the structure may cause catastrophic failure, destruction to life support systems and cause injuries and death. Secondary effects of explosion may even prevent or hinder evacuation of people from the structure thereby causing additional death and injuries. An extensive review of published literature in the present paper discusses parameters critically influencing structural and mechanical behavior with varying compressive strength, standoff distance, type of blast loading, and charge weight on UHPFRC structural elements. The following conclusions are drawn based on comprehensive analysis of the response of UHPFRC structural elements under flexural and compression members subjected to blast loading.

1. UHPFRCs have advantageous properties for resisting blast loading, and as such, composite can be utilized appropriately to prevent important buildings and human loss due to terrorist attacks.
2. The use of polypropylene fibers in concrete reduces about 70 and 50% damage at the top and bottom of the plates when subjected to a blast load of 15 kg TNT.
3. Shear failure has been observed as one of the primary modes of failure in UHPFRC during blast load at a close standoff distance. UHPFRC has a greater capacity to dissipate large amounts of energy during blast loading and shows superior performance than OSC and HSC.
4. Fiber reinforcement added to UHPFRC can affect failure and damage pattern, and blast behavior of elements without affecting structural integrity. Low-strength ductile fibers to UHPFRC have a minor impact on blast performance and fracture energy improvement.
5. For the protective design structures, high-strength composite materials like UHPFRC can be used with longi-

tudinal reinforcement. But the material has to be reinforced with steel.

6. The relationship between strain rate and dynamic amplification factor is insignificant. As a result, UHPFRC is preferred for application in blast-resistant structural elements.
7. UHPFRC can be beneficially utilized for blast-resistant constructions because it resists more than 400% force for the same size and reinforcement.
8. Experimental and analytical investigations by incorporating variables like standoff distance, charge weight, type of the blast, explosive and the material used, have been studied.

**Data availability** Some or all data, models, or code that support the findings of this study is available from the corresponding author upon reasonable request.

## Declarations

**Conflict of interest** On behalf of all authors, the corresponding author states that there is no conflict of interest.

**Ethical approval** The authors declare that they have not submitted the manuscript to any other journal for simultaneous consideration. The work is original and not published elsewhere.

## References

1. Wu C, Oehlers DJ, Rebenrost M, Leach J, Whittaker AS (2009) Blast testing of ultra-high performance fibre and FRP-retrofitted concrete slabs. *Eng Struct* 31:2060–2069. <https://doi.org/10.1016/j.engstruct.2009.03.020>
2. Rebenrost M, Wight G (2013) Investigation of UHPFRC Slabs Under Blast Loads, *Des. Build. with UHPFRC*:363–376
3. Habel K, Viviani M, Denarié E, Brühwiler E (2006) Development of the mechanical properties of an ultra-high performance fiber reinforced concrete (UHPFRC). *Cem Concr Res* 36:1362–1370. <https://doi.org/10.1016/j.cemconres.2006.03.009>
4. Graybeal BA (2007) Compressive behavior of ultra-high-performance fiber-reinforced concrete. *ACI Mater J* 104:146–152
5. Habel K, Gauvreau P (2008) Response of ultra-high performance fiber reinforced concrete (UHPFRC) to impact and static loading. *Cem Concr Compos* 30:938–946. <https://doi.org/10.1016/j.cemconcomp.2008.09.001>
6. Hassan AMT, Jones SW, Mahmud GH (2012) Experimental test methods to determine the uniaxial tensile and compressive behaviour of ultra-high performance fibre reinforced concrete (UHPFRC). *Constr Build Mater* 37:874–882. <https://doi.org/10.1016/j.conbuildmat.2012.04.030>
7. Tayeh BA, Bakar BHA, Johari MAM, Voo YL (2013) Utilization of ultra-high performance fibre concrete (UHPFC) for rehabilitation: a review. *Procedia Eng* 54:525–538. <https://doi.org/10.1016/j.proeng.2013.03.048>
8. Li J, Wu C, Hao H (2015) An experimental and numerical study of reinforced ultra-high performance concrete slabs under blast loads. *Mater Des* 82:64–76. <https://doi.org/10.1016/j.matdes.2015.05.045>
9. Li J, Wu C, Hao H, Su Y (2015) Investigation of ultra-high performance concrete under static and blast loads. *Int J Prot Struct* 6:217–235. <https://doi.org/10.1260/2041-4196.6.2.217>
10. Li J, Wu C, Hao H, Su Y, Li Z-X (2017) A study of concrete slabs with steel wire mesh reinforcement under close-in explosive loads. *Int J Impact Eng* 110:242–254. <https://doi.org/10.1016/j.ijimpeng.2017.01.016>
11. Mao L, Barnett SJ, Tyas A, Warren J, Schleyer GK, Zaini SS (2015) Response of small scale ultra high performance fibre reinforced concrete slabs to blast loading. *Constr Build Mater* 93:822–830. <https://doi.org/10.1016/j.conbuildmat.2015.05.085>
12. Xu J, Wu C, Xiang H, Su Y, Li Z-X, Fang Q, Hao H, Liu Z, Zhang Y, Li J (2016) Behaviour of ultra high performance fibre reinforced concrete columns subjected to blast loading. *Eng Struct* 118:97–107. <https://doi.org/10.1016/j.engstruct.2016.03.048>
13. Su V, Li J, Wu C, Wu P, Tao M, Li X (2017) Mesoscale study of steel fibre-reinforced ultra-high performance concrete under static and dynamic loads. *Mater Des* 116:340–351. <https://doi.org/10.1016/j.matdes.2016.12.027>
14. Kang S-H, Jeong Y, Tan KH, Moon J (2018) The use of limestone to replace physical filler of quartz powder in UHPFRC. *Cem Concr Compos* 94:238–247. <https://doi.org/10.1016/j.cemconcomp.2018.09.013>
15. Turker K, Hasgul U, Birol T, Yavas A, Yazici H (2019) Hybrid fiber use on flexural behavior of ultra high performance fiber reinforced concrete beams. *Compos Struct* 229:111400. <https://doi.org/10.1016/j.compstruct.2019.111400>
16. Song Q, Yu R, Shui Z, Rao S, Fan D, Gao X (2020) Macro/micro characteristics variation of ultra-high performance fibre reinforced concrete (UHPFRC) subjected to critical marine environments. *Constr Build Mater* 256:119458. <https://doi.org/10.1016/j.conbuildmat.2020.119458>
17. Chu SH, Li L, Shen PL, Lu JX, Poon CS (2022) Recycling of waste glass powder as paste replacement in green UHPFRC. *Constr Build Mater* 316:125719. <https://doi.org/10.1016/j.conbuildmat.2021.125719>
18. Lalwani SP, Gayner G (2020) Special report: India's Kashmir conundrum: before and after the abrogation of article 370, United States Institute of Peace, 2301 Constitution Avenue, NW Washington, DC 20037, 473:1–24
19. LaFree G, Dugan L, Fogg HV, Scott J (2006) Building a global terrorism database, National Institute of Justice, Office of Justice Programs, U.S. Department of Justice. 1–148
20. Goel MD, Matsagar VA (2014) Blast-resistant design of structures. *Am Soc Civ Eng* 19:04014007. [https://doi.org/10.1061/\(ASCE\)SC.1943-5576.0000188](https://doi.org/10.1061/(ASCE)SC.1943-5576.0000188)
21. Zhang C, Gholipour G, Mousavi AA (2020) Blast loads induced responses of RC structural members: state-of-the-art review. *Compos Part B Eng* 195:108066. <https://doi.org/10.1016/j.compositesb.2020.108066>
22. Karlos V, Solomos G (2013) Calculation of blast loads for application to structural components, JRC Technical report, EUR 26456 EN. <https://doi.org/10.2788/61866>
23. Samali B, McKenzie G, Zhang C, Ancich E (2018) Review of the basics of state of the art of blast loading. *Asian. J Civ Eng* 19:775–791. <https://doi.org/10.1007/s42107-018-0063-y>
24. Millard SG, Molyneaux TCK, Barnett SJ, Gao X (2010) Dynamic enhancement of blast-resistant ultra-high performance fibre-reinforced concrete under flexural and shear loading. *Int J Impact Eng* 37:405–413. <https://doi.org/10.1016/j.ijimpeng.2009.09.004>
25. Tedesco CARJW (1998) Strain-rate-dependent constitutive equations for concrete. *ASME* 120:398–405
26. Rong Z, Sun W, Zhang Y (2010) Dynamic compression behavior of ultra-high performance cement based composites. *Int J Impact Eng* 37:515–520. <https://doi.org/10.1016/j.ijimpeng.2009.11.005>

27. Yi N-H, Kim J-HJ, Han T-S, Cho Y-G, Lee JH (2012) Blast-resistant characteristics of ultra-high strength concrete and reactive powder concrete. *Constr Build Mater* 28:694–707. <https://doi.org/10.1016/j.conbuildmat.2011.09.014>
28. Maalej M, Quek ST, Zhang J (2005) Behavior of hybrid-fiber engineered cementitious composites subjected to dynamic tensile loading and projectile impact. *J Mater Civ Eng* 17:143–152. [https://doi.org/10.1061/\(ASCE\)0899-1561\(2005\)17:2\(143\)](https://doi.org/10.1061/(ASCE)0899-1561(2005)17:2(143))
29. Malvar LJ, Crawford JE (1998) Dynamic increase factors for concrete. In: 28th DDESB Semin. Orlando. 1–17
30. Hopkinson B (1915) British ordinance board minutes 13565, kew, UK, National Archives
31. Baker W (1973) *Explosion in air*. University of Texas Press, Austin
32. Department of Defense, Unified Facilities Criteria: Structures to resist the effects of accidental explosions (2008) UFC 3-340-02, Washington, DC
33. Kumar D, Elias AJ (2019) The explosive chemistry of nitrogen. *Resonance* 24:1253–1271. <https://doi.org/10.1007/s12045-019-0893-2>
34. Brode HL (1955) Numerical solutions of spherical blast waves. *J Appl Phys* 26:766–775. <https://doi.org/10.1063/1.1722085>
35. Henrych J, Major R (1979) *The dynamics of explosion and its use, developments in atmospheric science*. Elsevier, Amsterdam
36. Bajic M (1983) Blast waves in free air, propellants. *Explos Pyrotech* 8:1–7. <https://doi.org/10.1002/prop.19830080102>
37. Mills CA (1987) The design of concrete structure to resist explosions and weapon effects. In: *Proceedings of the 1st international conference for hazard protections*, 61–73
38. Sadovskiy MA (2004) Mechanical effects of air shockwaves from explosions according to experiments, MA selected works: geophysics and physics of explosion. Nauka Express, Moscow
39. Bajic Z (2007) Determination of TNT equivalent for various explosives, Masters Thesis, University of Belgrade, Belgrade, Serbia
40. Kinney GF, Graham KJ (1985) *Explosive shocks in air*. Springer Publishing Company, Berlin
41. US Army, Fundamental of Protective Design (Non-Nuclear) (1965) Department of Army Technical Manual, TM5-855-1, US Army, Washington, DC, USA
42. Newmark NM, Hansen RJ (1961) Design of blast resistant structures. In: Crede H (ed) *Shock and vibration handbook*. McGraw-Hill, New York, p 3
43. Wu C, Hao H (2005) Modeling of simultaneous ground shock and airblast pressure on nearby structures from surface explosions. *Int J Impact Eng* 31:699–717. <https://doi.org/10.1016/j.ijimpeng.2004.03.002>
44. Siddiqui JI, Ahmad S (2007) Impulsive loading on a concrete structure. *Proc Inst Civ Eng Struct Build* 160:231–241. <https://doi.org/10.1680/stbu.2007.160.4.231ol>
45. Ahmad S, Elahi A, Iqbal J, Keyani MA, Rahman AGA (2013) Impulsive loading on reinforced concrete wall. *Proc Inst Civ Eng Struct Build* 166:153–162. <https://doi.org/10.1680/stbu.11.00008>
46. Iqbal J, Ahmad S (2015) Improving safety provisions of structural design of containment against external explosion. In: *Proceedings of International conference on opportunities and challenges for water cooled reactors in the 21st century*. 1–5
47. Ngo T, Mendis P, Ramsay J (2007) Blast loading and blast effects on structures: an overview. *EJSE Spec Issue Load Struct* 1:76–91
48. Mahmud GH, Hassan AMT, Jones SW, Schleyer GK (2021) Experimental and numerical studies of ultra high performance fibre reinforced concrete (UHPC) two-way slabs. *Structures* 29:1763–1778. <https://doi.org/10.1016/j.istruc.2020.12.053>
49. Ha J-H, Yi N-H, Choi J-K, Kim J-HJ (2011) Experimental study on hybrid CFRP-PU strengthening effect on RC panels under blast loading. *Compos Struct* 93:2070–2082. <https://doi.org/10.1016/j.compstruct.2011.02.014>
50. Schleyer GK, Barnett SJ, Millard SG, Wight G (2010) Modelling the response of UHPC panels to explosive loading. *Struct Under Shock Impact XI*:173–184. <https://doi.org/10.2495/SU100151>
51. Du Y, Wei J, Liu K, Huang D, Lin Q, Yang B (2020) Research on dynamic constitutive model of ultra-high performance fiber-reinforced concrete. *Constr Build Mater* 234:117386. <https://doi.org/10.1016/j.conbuildmat.2019.117386>
52. Banerji S, Kodur V, Solhmirzaei R (2020) Experimental behavior of ultra high performance fiber reinforced concrete beams under fire conditions. *Eng Struct* 208:110316. <https://doi.org/10.1016/j.engstruct.2020.110316>
53. Astarlioglu S, Krauthammer T (2014) Response of normal-strength and ultra-high-performance fiber-reinforced concrete columns to idealized blast loads. *Eng Struct* 61:1–12. <https://doi.org/10.1016/j.engstruct.2014.01.015>
54. Ellis BD, DiPaolo BP, McDowell DL, Zhou M (2014) Experimental investigation and multiscale modeling of ultra-high-performance concrete panels subject to blast loading. *Int J Impact Eng* 69:95–103. <https://doi.org/10.1016/j.ijimpeng.2013.12.011>
55. Barnett SJ, Millard SG, Schleyer GK, Tyas A (2010) Briefing: blast tests of fibre-reinforced concrete panels. *Proc Inst Civ Eng Constr Mater* 163:127–129. <https://doi.org/10.1680/coma.900017>
56. Cavili B, Rebenstro M, Perry V (2006) Ductal: a high-performance material for resistance to blasts and impacts. *Aust J Struct Eng*. <https://doi.org/10.1080/13287982.2006.11464962>
57. Castedo R, Santos AP, Alañón A, Reifarth C, Chiquito M, López LM, Martínez-Almajano S, Pérez-Caldentey A (2021) Numerical study and experimental tests on full-scale RC slabs under close-in explosions. *Eng Struct* 231:111774. <https://doi.org/10.1016/j.engstruct.2020.111774>
58. Kadhim MMA, Jawdhari A, Peiris A (2021) Development of hybrid UHPC-NC beams: a numerical study. *Eng Struct* 233:111893. <https://doi.org/10.1016/j.engstruct.2021.111893>
59. Almustafa MK, Nehdi ML (2020) Machine learning model for predicting structural response of RC slabs exposed to blast loading. *Eng Struct* 221:111109. <https://doi.org/10.1016/j.engstruct.2020.111109>
60. Elvira MP, Lam N, Ngo T (2006) Progressive collapse analysis of RC frames subjected to blast loading. *Aust J Struct Eng* 7:47–55. <https://doi.org/10.1080/13287982.2006.11464963>
61. Lok TS, Xiao JR (1999) Steel-fibre-reinforced concrete panels exposed to air blast loading. *Proc Inst Civ Eng Struct Build* 134:319–331. <https://doi.org/10.1680/istbu.1999.31898>
62. Mays TARGC, Hetherington JG (1999) Response to blast loading of concrete wall panels with openings. *J Struct Eng* 125:1448–1450
63. Lan S, Lok T-S, Heng L (2005) Composite structural panels subjected to explosive loading. *Constr Build Mater* 19:387–395. <https://doi.org/10.1016/j.conbuildmat.2004.07.021>
64. Hoemann J, Salim H, Air T, Base F, Dinan RJ (2008) Fiber reinforced polymer (Frp) panels for blast and fragmentation mitigation airbase technologies division, AIR FORCE Res. Lab
65. Ngo T, Mendis P, Krauthammer T (2007) Behavior of ultrahigh-strength prestressed concrete panels subjected to blast loading. *J Struct Eng* 133:1582–1590. [https://doi.org/10.1061/\(ASCE\)0733-9445\(2007\)133:11\(1582\)](https://doi.org/10.1061/(ASCE)0733-9445(2007)133:11(1582))
66. Ohtsu M, Uddin FAKM, Tong W, Murakami K (2007) Dynamics of spall failure in fiber reinforced concrete due to blasting. *Constr Build Mater* 21:511–518. <https://doi.org/10.1016/j.conbuildmat.2006.04.007>
67. Ghani Razaqpur A, Tolba A, Contestabile E (2007) Blast loading response of reinforced concrete panels reinforced



- with externally bonded GFRP laminates. *Compos Part B Eng* 38:535–546. <https://doi.org/10.1016/j.compositesb.2006.06.016>
68. Silva PF, Lu B (2007) Improving the blast resistance capacity of RC slabs with innovative composite materials. *Compos Part B Eng* 38:523–534. <https://doi.org/10.1016/j.compositesb.2006.06.015>
  69. Schenker A, Anteby I, Gal E, Kivity Y, Nizri E, Sadot O, Michaelis R, Levitant O, Ben-Dor G (2007) Full-scale field tests of concrete slabs subjected to blast loads. *Int J Impact Eng* 35:84–198. <https://doi.org/10.1016/j.ijimpeng.2006.12.008>
  70. Zhou XQ, Kuznetsov VA, Hao H, Waschl J (2008) Numerical prediction of concrete slab response to blast loading. *Int J Impact Eng* 35:1186–1200. <https://doi.org/10.1016/j.ijimpeng.2008.01.004>
  71. Wu C, Nurwidayati R, Oehlers DJ (2009) Fragmentation from spallation of RC slabs due to airblast loads. *Int J Impact Eng* 36:1371–1376. <https://doi.org/10.1016/j.ijimpeng.2009.03.014>
  72. Beppu M, Ohno T, Ohkubo K, Li B, Satoh K (2010) Contact explosion resistance of concrete plates externally strengthened with FRP laminates. *Int J Prot Struct* 1:257–270. <https://doi.org/10.1260/2041-4196.1.2.257>
  73. Urgessa GS, Maji AK (2010) Dynamic response of retrofitted masonry walls for blast loading. *J Eng Mech* 136:858–864. [https://doi.org/10.1061/\(ASCE\)JEM.1943-7889.0000128](https://doi.org/10.1061/(ASCE)JEM.1943-7889.0000128)
  74. Yusof M, Norazman N (2010) Normal strength steel fiber reinforced concrete subjected to explosive loading. *Int J Sustain Eng Technol* 1:127–136
  75. Garfield TT, Richins WD, Larson TK, Pantelides CP, Blakeley JE (2011) Performance of RC and FRC wall panels reinforced with mild steel and GFRP composites in blast events. *Procedia Eng* 10:3534–3539. <https://doi.org/10.1016/j.proeng.2011.04.581>
  76. Morales-Alonso G, Cendón DA, Gálvez F, Erice B, Sánchez-Gálvez V (2011) Blast response analysis of reinforced concrete slabs: experimental procedure and numerical simulation. *J Appl Mech* 78:1–13. <https://doi.org/10.1115/1.4004278>
  77. Wu C, Huang L, Oehlers DJ (2011) Blast testing of aluminum foam-protected reinforced concrete slabs. *J Perform Constr Facil* 25:464–474. [https://doi.org/10.1061/\(ASCE\)CF.1943-5509.0000163](https://doi.org/10.1061/(ASCE)CF.1943-5509.0000163)
  78. Yamaguchi M, Murakami K, Takeda K, Mitsui Y (2011) Blast resistance of double-layered reinforced concrete slabs composed of precast thin plates. *J Adv Concr Technol* 9:177–191. <https://doi.org/10.3151/jact.9.177>
  79. Foglar M, Kovar M (2013) Conclusions from experimental testing of blast resistance of FRC and RC bridge decks. *Int J Impact Eng* 59:18–28. <https://doi.org/10.1016/j.ijimpeng.2013.03.008>
  80. Tabatabaei ZS, Volz JS, Baird J, Gliha BP, Keener DI (2013) Experimental and numerical analyses of long carbon fiber reinforced concrete panels exposed to blast loading. *Int J Impact Eng* 57:70–80. <https://doi.org/10.1016/j.ijimpeng.2013.01.006>
  81. Chen L, Fang Q, Fan J, Zhang Y, Hao H, Liu J (2014) Responses of masonry infill walls retrofitted with CFRP, steel wire mesh and laminated bars to blast loadings. *Adv Struct Eng* 17:817–836. <https://doi.org/10.1260/1369-4332.17.6.817>
  82. Mao L, Barnett S, Begg D, Schleyer G, Wight G (2014) Numerical simulation of ultra-high performance fibre reinforced concrete panel subjected to blast loading. *Int J Impact Eng* 64:91–100. <https://doi.org/10.1016/j.ijimpeng.2013.10.003>
  83. Orton SL, Chiarito VP, Minor JK, Coleman TG (2014) Experimental testing of CFRP-strengthened reinforced concrete slab elements loaded by close-in blast. *J Struct Eng* 140:04013060. [https://doi.org/10.1061/\(ASCE\)ST.1943-541X.0000821](https://doi.org/10.1061/(ASCE)ST.1943-541X.0000821)
  84. Castedo R, Segarra P, Alañón A, Lopez LM, Santos AP, Sanchidrian JA (2015) Air blast resistance of full-scale slabs with different compositions: Numerical modeling and field validation. *Int J Impact Eng* 86:145–156. <https://doi.org/10.1016/j.ijimpeng.2015.08.004>
  85. Foglar M, Hajek R, Kovar M, Štoller J (2015) Blast performance of RC panels with waste steel fibers. *Constr Build Mater* 94:536–546. <https://doi.org/10.1016/j.conbuildmat.2015.07.082>
  86. Li J, Wu C, Hao H (2015) Investigation of ultra-high performance concrete slab and normal strength concrete slab under contact explosion. *Eng Struct* 102:395–408. <https://doi.org/10.1016/j.engstruct.2015.08.032>
  87. Alengaram UJ, Mohottige NHW, Wu C, Jumaat MZ, Poh YS, Wang Z (2016) Response of oil palm shell concrete slabs subjected to quasi-static and blast loads. *Constr Build Mater* 116:391–402. <https://doi.org/10.1016/j.conbuildmat.2016.04.103>
  88. Alysad SH, Elsanadedy HM, Al-Zaheri ZM, Al-Salloum YA, Abbas H (2016) Blast response of GFRP-strengthened infill masonry walls. *Constr Build Mater* 115:438–451. <https://doi.org/10.1016/j.conbuildmat.2016.04.053>
  89. Li J, Wu C, Hao H, Su Y, Liu Z (2016) Blast resistance of concrete slab reinforced with high performance fibre material. *J Struct Integr Maint* 1:51–59. <https://doi.org/10.1080/24705314.2016.1179496>
  90. Li J, Wu C, Hao H, Wang Z, Su Y (2016) Experimental investigation of ultra-high performance concrete slabs under contact explosions. *Int J Impact Eng* 93:62–75. <https://doi.org/10.1016/j.ijimpeng.2016.02.007>
  91. Oña M, Morales-Alonso G, Gálvez F, Sánchez-Gálvez V, Cendón D (2016) Analysis of concrete targets with different kinds of reinforcements subjected to blast loading. *Eur Phys J Spec Top* 225:265–282. <https://doi.org/10.1140/epjst/e2016-02633-8>
  92. Xia Y, Wu C, Liu Z-X, Yuan Y (2016) Protective effect of graded density aluminium foam on RC slab under blast loading: an experimental study. *Constr Build Mater* 111:209–222. <https://doi.org/10.1016/j.conbuildmat.2016.02.092>
  93. Zhai C, Chen L, Xiang H, Fang Q (2016) Experimental and numerical investigation into RC beams subjected to blast after exposure to fire. *Int J Impact Eng* 97:29–45. <https://doi.org/10.1016/j.ijimpeng.2016.06.004>
  94. Bibora P, Drdlová M, Prachař V, Sviták O (2017) UHPC for blast and ballistic protection, explosion testing and composition optimization. *IOP Conf Ser Mater Sci Eng* 251:012004. <https://doi.org/10.1088/1757-899X/251/1/012004>
  95. Foglar M, Hajek R, Fladr J, Pachman J, Stoller J (2017) Full-scale experimental testing of the blast resistance of HPRC and UHPFRC bridge decks. *Constr Build Mater* 145:588–601. <https://doi.org/10.1016/j.conbuildmat.2017.04.054>
  96. Li Z, Chen L, Fang Q, Chen W, Hao H, Zhang Y (2017) Experimental and numerical study of basalt fiber reinforced polymer strip strengthened autoclaved aerated concrete masonry walls under vented gas explosions. *Eng Struct* 152:901–919. <https://doi.org/10.1016/j.engstruct.2017.09.055>
  97. Luccioni B, Isla F, Codina R, Ambrosini D, Zerbino R, Giaccio G, Torrijos MC (2017) Effect of steel fibers on static and blast response of high strength concrete. *Int J Impact Eng* 107:23–37. <https://doi.org/10.1016/j.ijimpeng.2017.04.027>
  98. Wang J, Ren H, Wu X, Cai C (2017) Blast response of polymer-retrofitted masonry unit walls. *Compos Part B Eng* 128:174–181. <https://doi.org/10.1016/j.compositesb.2016.02.044>
  99. Wu C, Li J (2017) Structural protective design with innovative concrete material and retrofitting technology. *Procedia Eng* 173:49–56. <https://doi.org/10.1016/j.proeng.2016.12.020>
  100. Choi J-H, Choi S-J, Kim J-HJ, Hong K-N (2018) Evaluation of blast resistance and failure behavior of prestressed concrete under blast loading. *Constr Build Mater* 173:550–572. <https://doi.org/10.1016/j.conbuildmat.2018.04.047>
  101. Hajek R, Fladr J, Pachman J, Stoller J, Foglar M (2019) An experimental evaluation of the blast resistance of heterogeneous



- concrete-based composite bridge decks. *Eng Struct* 179:204–210. <https://doi.org/10.1016/j.engstruct.2018.10.070>
102. Liao Z, Li ZZ, Xue YL, Shao LZ, Yang DP, Tang DG (2019) Study on anti-explosion behavior of high-strength reinforced concrete beam under blast loading. *Strength Mater* 51:926–938. <https://doi.org/10.1007/s11223-020-00143-4>
  103. Peng Y, Wu C, Li J, Liu J, Liang X (2019) Mesoscale analysis on ultra-high performance steel fibre reinforced concrete slabs under contact explosions. *Compos Struct* 228:111322. <https://doi.org/10.1016/j.compstruct.2019.111322>
  104. Zhao C, Lu X, Wang Q, Gautam A, Wang J, Mo YL (2019) Experimental and numerical investigation of steel-concrete (SC) slabs under contact blast loading. *Eng Struct* 196:109337. <https://doi.org/10.1016/j.engstruct.2019.109337>
  105. Yang F, Feng W, Liu F, Jing L, Yuan B, Chen D (2019) Experimental and numerical study of rubber concrete slabs with steel reinforcement under close-in blast loading. *Constr Build Mater* 198:423–436. <https://doi.org/10.1016/j.conbuildmat.2018.11.248>
  106. Wu J, Zhou Y, Zhang R, Liu C, Zhang Z (2020) Numerical simulation of reinforced concrete slab subjected to blast loading and the structural damage assessment. *Eng Fail Anal* 118:104926. <https://doi.org/10.1016/j.engfailanal.2020.104926>
  107. Kumar V, Kartik KV, Iqbal MA (2020) Experimental and numerical investigation of reinforced concrete slabs under blast loading. *Eng Struct* 206:110125. <https://doi.org/10.1016/j.engstruct.2019.110125>
  108. Li Y, Chen Z, Ren X, Tao R, Gao R, Fang D (2020) Experimental and numerical study on damage mode of RC slabs under combined blast and fragment loading. *Int J Impact Eng* 142:103579. <https://doi.org/10.1016/j.ijimpeng.2020.103579>
  109. Lee J-Y, Aoude H, Yoon Y-S, Mitchell D (2020) Impact and blast behavior of seismically-detailed RC and UHPFRC-Strengthened columns. *Int J Impact Eng* 143:103628. <https://doi.org/10.1016/j.ijimpeng.2020.103628>
  110. Shaikh FUA, Luhar S, Arel HŞ, Luhar I (2020) Performance evaluation of Ultrahigh performance fibre reinforced concrete: a review. *Constr Build Mater* 232:17152. <https://doi.org/10.1016/j.conbuildmat.2019.117152>
  111. Buttignol TET, Sousa JLAO, Bittencourt TN (2017) Ultra High-Performance Fiber-Reinforced Concrete (UHPFRC): a review of material properties and design procedures. *Rev IBRACON Estruturas e Mater* 10:957–971. <https://doi.org/10.1590/s1983-41952017000400011>
  112. Remennikov A, Carolan D (2006) Blast effects and vulnerability of building structures from terrorist attack. *Aust J Struct Eng* 7:1–11. <https://doi.org/10.1080/13287982.2006.11464959>
  113. Dragani H, Sigmund V (2012) Blast loading on structures. *Tech Gazette* 19:643–652
  114. Hao H, Li Z-X, Shi Y (2016) Reliability analysis of RC columns and frame with FRP strengthening subjected to explosive loads. *J Perform Constr Facil* 30:04015017. [https://doi.org/10.1061/\(ASCE\)CF.1943-5509.0000748](https://doi.org/10.1061/(ASCE)CF.1943-5509.0000748)
  115. Fujikura S, Bruneau M, Lopez-Garcia D (2008) Experimental investigation of multihazard resistant bridge piers having concrete-filled steel tube under blast loading. *J Bridg Eng* 13:586–594. [https://doi.org/10.1061/\(ASCE\)1084-0702\(2008\)13:6\(586\)](https://doi.org/10.1061/(ASCE)1084-0702(2008)13:6(586))
  116. Fujikura S, Bruneau M (2011) Experimental investigation of seismically resistant bridge piers under blast loading. *J Bridg Eng* 16:63–71. [https://doi.org/10.1061/\(ASCE\)1084-0702\(2008\)13:6\(586\)](https://doi.org/10.1061/(ASCE)1084-0702(2008)13:6(586))
  117. Wu K-C, Li B, Tsai K-C (2011) The effects of explosive mass ratio on residual compressive capacity of contact blast damaged composite columns. *J Constr Steel Res* 67:602–612. <https://doi.org/10.1016/j.jcsr.2010.12.001>
  118. Fujikake K, Aemlaor P (2013) Damage of reinforced concrete columns under demolition blasting. *Eng Struct* 55:116–125. <https://doi.org/10.1016/j.engstruct.2011.08.038>
  119. Roller C, Mayrhofer C, Riedel W, Thoma K (2013) Residual load capacity of exposed and hardened concrete columns under explosion loads. *Eng Struct* 55:66–72. <https://doi.org/10.1016/j.engstruct.2011.12.004>
  120. Codina R, Ambrosini D, de Borbón F (2016) Alternatives to prevent the failure of RC members under close-in blast loadings. *Eng Fail Anal* 60:96–106. <https://doi.org/10.1016/j.engfailanal.2015.11.038>
  121. Fouché P, Bruneau M, Chiarito VP (2016) Modified steel-jacketed columns for combined blast and seismic retrofit of existing bridge columns. *J Bridg Eng* 21:04016035. [https://doi.org/10.1061/\(ASCE\)BE.1943-5592.0000882](https://doi.org/10.1061/(ASCE)BE.1943-5592.0000882)
  122. Zhang F, Wu C, Zhao X-L, Xiang H, Li Z-X, Fang Q, Liu Z, Zhang Y, Heidarpour A, Packer JA (2016) Experimental study of CFDST columns infilled with UHPC under close-range blast loading. *Int J Impact Eng* 93:184–195. <https://doi.org/10.1016/j.ijimpeng.2016.01.011>
  123. Li J, Wu C, Hao H, Liu Z (2017) Post-blast capacity of ultra-high performance concrete columns. *Eng Struct* 134:289–302. <https://doi.org/10.1016/j.engstruct.2016.12.057>
  124. Yuan S, Hao H, Zong Z, Li J (2017) A study of RC bridge columns under contact explosion. *Int J Impact Eng* 109:378–390. <https://doi.org/10.1016/j.ijimpeng.2017.07.017>
  125. Codina R, Ambrosini D, de Borbón F (2017) New sacrificial cladding system for the reduction of blast damage in reinforced concrete structures. *Int J Prot Struct* 8:221–236. <https://doi.org/10.1177/2041419617701571>
  126. Li M, Zong Z, Liu L, Lou F (2018) Experimental and numerical study on damage mechanism of CFDST bridge columns subjected to contact explosion. *Eng Struct* 159:265–276. <https://doi.org/10.1016/j.engstruct.2018.01.006>
  127. Rajkumar D, Senthil R, Bala Murali Kumar B, AkshayaGomathi K, Mahesh Velan S (2020) Numerical study on parametric analysis of reinforced concrete column under blast loading. *J Perform Constr Facil* 34:04019102. [https://doi.org/10.1061/\(ASCE\)CF.1943-5509.0001382](https://doi.org/10.1061/(ASCE)CF.1943-5509.0001382)
  128. Wang J, Yuan W, Feng R, Guo J, Dang X (2020) Dynamic performances of ultra-high-performance fiber-reinforced concrete-strengthened concrete columns subjected to blast impacts. *Adv Struct Eng* 23:3009–3023. <https://doi.org/10.1177/1369433220924797>

Springer Nature or its licensor holds exclusive rights to this article under a publishing agreement with the author(s) or other rightsholder(s); author self-archiving of the accepted manuscript version of this article is solely governed by the terms of such publishing agreement and applicable law.